Targeting Senescent Cells Enhances Adipogenesis and Metabolic Function in Old Age

Ming Xu[1,2], Allyson K. Palmer[1,2], Husheng Ding[1], Megan M. Weivoda[1], Tamar Pirtskhalava[1], Thomas A. White[1], Anna Sepe[1], Kurt O. Johnson[1], Michael B. Stout[1], Nino Giorgadze[1], Michael D. Jensen[1], Nathan K. LeBrasseur[1], Tamar Tchkonia[1], James L. Kirkland[1]*

[1]Robert and Arlene Kogod Center on Aging, Mayo Clinic, Rochester, MN

[2]These authors contributed equally to this work.

*To whom correspondence should be addressed at:

James L. Kirkland, M.D., Ph.D.,

Mayo Clinic Robert and Arlene Kogod Center on Aging,

200 First Street, S.W.,

Rochester MN 55905

Telephone: 1 507 266-9151

Email: Kirkland.James@mayo.edu

16 **Competing Interests Statement**

17 JLK, TT, TP, NG, and AKP have a financial interest related to this research. This research has
18 been reviewed by the Mayo Clinic Conflict of Interest Review Board and is being conducted in
19 compliance with Mayo Clinic Conflict of Interest policies.

20

Abstract

Senescent cells accumulate in fat with aging. We previously found genetic clearance of senescent cells from progeroid INK-ATTAC mice prevents lipodystrophy. Here we show that primary human senescent fat progenitors secrete activin A and directly inhibit adipogenesis in non-senescent progenitors. Blocking activin A partially restored lipid accumulation and expression of key adipogenic markers in differentiating progenitors exposed to senescent cells. Mouse fat tissue activin A increased with aging. Clearing senescent cells from 18-month-old naturally-aged INK-ATTAC mice reduced circulating activin A, blunted fat loss, and enhanced adipogenic transcription factor expression within 3 weeks. JAK inhibitor suppressed senescent cell activin A production and blunted senescent cell-mediated inhibition of adipogenesis. Eight weeks-treatment with ruxolitinib, an FDA-approved JAK1/2 inhibitor, reduced circulating activin A, preserved fat mass, reduced lipotoxicity, and increased insulin sensitivity in 22-month-old mice. Our study indicates targeting senescent cells or their products may alleviate age-related dysfunction of progenitors, adipose tissue, and metabolism.

35 **Introduction**

36 A major function of adipose tissue is to store potentially cytotoxic lipids, including fatty
37 acids (FAs), as less reactive neutral triglycerides (TG) within fat droplets[1]. Lipid storage by
38 adipose tissue appears to constitute a defense against lipotoxicity and metabolic disease[2-5]. Fat
39 cells turn over throughout life, with generation of new fat cells through differentiation of fat
40 progenitors (also known as preadipocytes or adipose-derived stem cells)[6,7,8]. Adipogenesis is
41 orchestrated by a transcription factor cascade involving the two key regulators, peroxisome
42 proliferator-activated receptor-γ (PPARγ) and CCAAT/enhancer binding protein-α (C/EBPα)[9,10]
43 and their downstream targets, including fatty acid binding protein 4 (*FABP4*) and perilipin
44 (*PLIN1*)[11,12]. Compromised adipogenic capacity can contribute to impaired ability of adipose
45 tissue to store lipids, leading to FA spillover and ectopic lipid accumulation in liver and other
46 sites, insulin resistance, and lipotoxicity [13,14-16]. By late middle age, capacity for adipogenesis,
47 *PPARγ* and *C/EBPα* expression, adipose tissue mass, and metabolic function begin to decline in
48 experimental animals and humans[5,14,17-28]. This age-related lipodystrophy likely contributes to
49 the pathogenesis of metabolic dysfunction at older ages[4,5,15,16,24].

50 We hypothesize that cellular senescence could contribute to impaired adipogenesis and
51 age-related lipodystrophy[5]. Cellular senescence refers to an essentially irreversible arrest of cell
52 proliferation[29]. It can be induced by a variety of stresses, including DNA damage, telomere
53 shortening, radiation, chemotherapeutics, and reactive metabolites[18,30]. Senescent cells
54 accumulate in adipose tissue with aging across a number of mammalian species[5,31,32] and secrete
55 an array of cytokines, chemokines, proteases, and growth factors – the senescence-associated
56 secretory phenotype (SASP)[33,34]. Cultures of progenitors isolated from adipose depots of older
57 animals or humans contain senescent cells and exhibit impaired adipogenic capacity, with

58 reduced lipid accumulation and C/EBPα and PPARγ expression after exposure to differentiation-
59 inducing stimuli [5,26,35,36]. Senescent cells appear to be able to spread inflammatory activation and
60 perhaps even senescence to nearby non-senescent cells[31,37,38]. In previous work, we used a
61 genetically modified INK-ATTAC (*Cdkn2a /p16*^{Ink4a} promoter driven apoptosis through targeted
62 activation of caspase) mouse model to selectively eliminate *Cdkn2a* (*p16*^{Ink4a}) positive senescent
63 cells through apoptosis by the administration of AP20187, a drug that induces dimerization of a
64 membrane-bound myristoylated FK506 binding protein fused with caspase 8 (FKBP–Casp8)[39].
65 We showed that clearance of senescent cells can delay age-related phenotypes including
66 lordokyphosis and cataract formation, and can actually reverse age-related fat loss in progeroid
67 *BubR1*$^{H/H}$ animals[39], implicating senescent cells as a driver of age-related phenotypes.
68 Furthermore, interleukin-6 (IL6)[40,41], tumor necrosis factor α (TNFα)[26,40,41], and interferon γ
69 (IFNγ)[42] can inhibit adipogenesis *in vitro*. These factors are among the SASP components in
70 senescent fat progenitors and other senescent cell types[18,31,33,34]. However, causal links between
71 these paracrine factors and impaired adipogenesis related to cellular senescence have not been
72 demonstrated. We recently reported that the JAK/STAT (Janus kinase/signal transducer and
73 activator of transcription) pathway plays a role in regulating the SASP[31]. Therefore, we
74 hypothesized that JAK inhibition might rescue impaired adipogenesis due to senescent cells and
75 thus preserve fat mass and metabolic function in older individuals.

76 We report here that senescent fat progenitors impede differentiation of non-senescent
77 progenitors, in part by secreting activin A, a member of the transforming growth factor
78 superfamily, which can inhibit adipogenesis and interfere with stem cell and progenitor
79 function[43]. Eliminating senescent cells from naturally-aged INK-ATTAC mice reduced activin A
80 and increased adipose tissue *C/EBPα* and *PPARγ*. JAK pathway inhibition suppressed production

81 of activin A by senescent fat progenitors and partially rescued adipogenic capacity both *in vitro*
82 and *in vivo*. JAK inhibition in aged mice reduced lipotoxicity and increased insulin sensitivity.
83 Our findings provide new insights into the mechanisms of age-related progenitor dysfunction, fat
84 loss, and metabolic dysfunction, as well as potential therapeutic avenues for preventing or
85 alleviating these common conditions.

Results

Senescent fat cell progenitors impede adipogenesis. To determine if senescent cells influence adipogenesis in adjacent non-senescent cells, we devised a co-culture system with non-senescent human primary fat progenitors as "target" cells and either senescent or non-senescent human progenitors as "source" cells. Primary cells were isolated from the stromal-vascular fraction of collagenase-digested subcutaneous fat from healthy human subjects undergoing surgery to donate a kidney. Cells were passaged 4-6 times under conditions to enrich for fat progenitors as opposed to endothelial cells or macrophages[6]. These cells were exposed to 10 Gy irradiation, which induced at least 70% of cells to become senescence-associated β-galactosidase (SABG)-positive within 20 days, as previously described[31]. Target cells were distinguished from source cells by fluorescent labeling (CM-DiI), which does not independently affect adipogenesis. We differentiated the mixture of cells using an adipogenic differentiation medium (DM) for 15 days. Differentiation was assessed by examining lipid accumulation inside the cells. We considered a cell to be differentiated if it contained doubly refractile lipid droplets visible by low power phase contrast microscopy, a change that occurs in fat cell progenitors following DM exposure, but not in other cell types[44]. We found that senescent source cells were less differentiated than control non-senescent source cells (Figure 1a). When co-cultured with senescent source cells, only 20% of target progenitors accumulated lipid compared to more than 50% when co-cultured with non-senescent source cells (Figure 1b), indicating that senescent cells can directly impair lipid accumulation by nearby fat progenitors.

Next, we examined the nature of the factors responsible for impairing adipogenesis. Non-senescent progenitors were treated with DM in the presence of conditioned medium (CM) from cultures of senescent or non-senescent cells. Senescent progenitor CM reduced differentiated cell

109 numbers in target non-senescent cells at all three time points tested (Figure 2a). PPARγ, C/EBPα,
110 FABP4, and PLIN2 are normally up-regulated during adipogenesis[9-12]. Differentiation-dependent
111 expression of these genes was blunted by CM from senescent cells compared to CM from blank
112 culture flasks or control non-senescent cells (Figure 2b). Cellular senescence did not appear to be
113 induced in the target cells by the 15 days of CM exposure, since $p16^{Ink4a}$ and *Cdkn1a* ($p21^{Cip}$)
114 transcript levels were not increased (Figure 2-figure supplement. 1a). Adipogenesis was not
115 impaired when exposure to CM was limited to 24 hours of pretreatment before exposure to DM
116 (Figure 2-figure supplement. 1b). This suggests that impaired adipogenesis due to senescent CM
117 depends on continued presence of products secreted by senescent cells. CM from doxorubicin-
118 induced senescent cells suppressed adipogenesis similarly to CM from irradiation-induced
119 senescent cells (Figure 2-figure supplement. 1c).

120 **Inhibition of activin A rescues impaired adipogenesis due to senescent CM.** We next
121 investigated which factors secreted by senescent cells impair adipogenesis. We found that CM
122 from senescent cells inhibited adipogenesis even after freeze-thaw cycles (Figure 2a, b).
123 Therefore, cell-cell contact or molecules with short half-lives, including many metabolites such
124 as reactive oxygen species (ROS), do not appear to be the sole responsible factors. CM from
125 senescent cells was separated into two fractions using molecular size filters with a cutoff at
126 ~10kd. The fraction larger than ~10kd impaired adipogenesis while the fraction smaller than
127 ~10kd had no effect (Figure 2-figure supplement 1d). This led us to hypothesize SASP peptides
128 or proteins might play a role in the inhibition of adipogenesis. Using either neutralizing
129 antibodies or specific inhibitors, we inhibited candidate SASP factors in the CM, including IL6,
130 TNFα, IFN γ, and activin A, which can be secreted by senescent cells and inhibit adipogenesis
131 [26,31,40-43] (Figure 2- figure supplement 1e). Among the compounds screened, SB-431542, an

132 activin A receptor inhibitor[45], substantially improved adipogenesis in progenitors exposed to CM
133 from senescent cells, while only slightly increasing adipogenesis in control cells (Figure 3a,b).
134 Due to the fact that SB-431542 also inhibits TGFβ signaling[45], to confirm further the role of
135 activin A, we used activin A-specific neutralizing antibody and observed a similar enhancement
136 of adipogenesis (Figure 3c,d). Together, these findings indicate that activin A plays a role in the
137 impairment of adipogenesis by senescent cells.

138 **Genetic clearance of senescent cells blunts fat loss and increases adipogenesis in 18-**
139 **month-old mice.** After 17-18 months-of-age, mice begin to lose fat mass. We previously found
140 that senescent cells start to accumulate noticeably before 18 months-of-age in mouse fat tissue[32]
141 and senescent cells play a role in age-related loss of subcutaneous fat in animals with progeria[39].
142 However, it is still unknown whether senescent cell clearance has effect on age-related adipose
143 phenotypes in naturally aged mice. To test this, we treated late middle-aged (18-month-old)
144 INK-ATTAC$^{+/-}$ and wild-type (WT) littermates with two 3-day courses of AP20187, with 14
145 days between treatments, for 3 weeks (total 6 days of treatment) to activate the caspase-8 moiety
146 in the *ATTAC* suicide gene product that is expressed only in *p16*^{Ink4a} positive senescent cells. This
147 allowed us to investigate the short-term response to senescent cell clearance, for example effects
148 on adipogenic transcription factors, and to reduce effects of possible long-term compensatory
149 responses. During the three-week treatment period, WT mice lost more fat than INK-ATTAC$^{+/-}$
150 mice (Figure 4a), while lean mass (Figure 4b) and total body weight (Figure 4c) were unaffected.
151 Circulating activin A was reduced more than 30% compared to baseline in the INK-ATTAC$^{+/-}$
152 mice, while activin A increased by 10% in the WT group (Figure 4e). Activin A was also
153 reduced in adipose tissue of the INK-ATTAC$^{+/-}$ mice (Figure 4f). Adipose tissue expression of
154 C/EBPα and PPARγ was higher in the INK-ATTAC$^{+/-}$ than WT mice (Figure 4f), indicating of

155 improved adipogenesis. Lipin-1, whose expression in fat tissue is positively associated with
156 adipose tissue function[46] and insulin sensitivity[47], was also increased in the INK-ATTAC$^{+/-}$ mice
157 (Figure 4f). The senescence markers, *IL6*, *p16*^{Ink4a}, and *p21*^{Cip1} (Figure 4f) as well as SABG^{+}
158 cells (Figure 4d and Figure 4-figure supplement 1), were reduced in fat tissue of AP20187-
159 treated INK-ATTAC$^{+/-}$ mice. These results suggest that senescent cells are a cause of age-related
160 adipose tissue loss and dysfunction in older mice.

161 **JAK inhibition reduces activin A production in senescent progenitors and partially**
162 **rescues adipogenesis.** We recently reported that JAK inhibition suppresses SASP factors,
163 including IL6 and TNFα, in senescent fat progenitors [31]. We also previously observed that direct
164 addition of recombinant activin A to cultured human fat progenitors impedes adipogenesis[43].
165 Here, we found that JAK inhibition reduces activin A at both the transcript (Figure 5a) and
166 secreted protein levels (Figure 5b) in senescent fat progenitors. We therefore tested whether JAK
167 inhibition alleviates impaired adipogenesis related to senescence. CM prepared from senescent
168 progenitors exposed to JAK inhibitor caused less inhibition of adipogenesis in non-senescent
169 target progenitors than CM prepared from senescent cells exposed to vehicle (Figure 5c,d). Since
170 JAK inhibitor was present in the CM, we examined whether the improvement of adipogenesis in
171 the target non-senescent cells was due to the effect of JAK inhibitor on the senescent source cells
172 or if JAK inhibitor had direct effects on the target cells. Addition of JAK inhibitor directly to CM
173 previously collected from either control or senescent cells did not affect adipogenesis in the
174 target non-senescent cells (Figure 5-figure supplement 1a). This indicates that JAK inhibitor
175 alleviated impaired adipogenesis mainly by acting on the senescent source fat progenitors, in turn
176 altering the composition of the CM, rather than having direct effects on the target cells.
177 Moreover, JAK inhibition improved adipogenesis in cultures of fat progenitors isolated from

178 aged rats, which contain senescent cells, but not in cultured progenitors isolated from young rats
179 (Figure 5-figure supplement 1b and c).

180 **JAK inhibition enhances adipogenesis and prevents fat loss in old mice.** To test
181 effects of JAK inhibition *in vivo*, we treated 22-24 month-old C57BL/6 male mice with
182 ruxolitinib (INCB), a selective JAK1/2 inhibitor approved by the FDA, or vehicle (DMSO) for 2
183 months. Vehicle-treated mice progressively lost fat over two months, while JAK inhibitor
184 administration prevented this age-related fat loss (Figure 6a,d). The lean mass of both groups
185 remained unchanged (Figure 6b,e). The body weights of the vehicle-treated compared to the
186 INCB-treated mice was not significantly different (Figure 6c,f). This was consistent in two
187 independent cohorts of mice using the same treatment regimen. Inguinal, subscapular, and brown
188 fat mass were reduced in the vehicle-treated group, but were preserved in INCB-treated mice
189 (Figure 7a). The same INCB treatment only exhibited a non-significant trend to alter fat mass in
190 young (8-month-old) mice (Figure 6-figure supplement 2a).

191 We next examined the mechanism of fat mass preservation due to JAK inhibition. JAK
192 inhibition increased adipose tissue transcript levels of the adipogenesis markers, *PPARγ, C/EBPα,*
193 *FABP4, and adipo-Q*, as well as *GPAT4* (glycerol-3-phosphate acyltransferase isoform-4, a TG
194 synthesis marker) (Figure 7b), suggesting that JAK inhibition may act by enhancing
195 adipogenesis and increasing TG storage in fat in aged mice. *Lipin-1* was also increased in fat
196 tissue from JAK inhibitor-treated mice (Figure 7b). Activin A increased with aging in both fat
197 tissues (Figure 6-figure supplement 2c) and the circulation (Figure 7c). JAK inhibition
198 suppressed *activin A* in both whole fat (Figure 7b) and progenitors isolated from fat tissue
199 (Figure 7-figure supplement 1), as well as circulating activin A (Figure 7c). Notably, JAK
200 inhibition did not reduce *activin A* expression or improve adipogenesis in fat tissue of younger

201 (8-month old) mice (Figure 6-figure supplement 2b). We also examined other potential causes of
202 preservation of fat mass by JAK inhibition. Administering JAK inhibitor did not change
203 metabolic rate or food intake in aged mice (Figure 6-figure supplement 1), and was previously
204 found by us to actually increase activity of old mice[31]. Expression of two lipolytic enzymes,
205 adipose triglyceride lipase (*ATGL*) and hormone-sensitive lipase (*HSL*), was induced in fat tissue
206 by JAK inhibition (Figure 7b). This suggests that the fat maintenance we observed was not due
207 to increased food intake, decreased energy expenditure, or decreased lipolysis. Next, we
208 examined whether increased adipogenic capacity was associated with suppressed FA spillover
209 and ectopic lipid accumulation. Plasma free fatty acid (FFA) levels were reduced by JAK
210 inhibitor (Figure 7e), while TG was not different (Figure7d). In addition, JAK inhibitor
211 decreased both liver weight (Figure 7a) and hepatic TG (Figure 7f,g) in old mice.

212 **JAK inhibition enhances metabolic function in old mice.** Lipotoxicity and decreased
213 adipogenic capacity are associated with insulin resistance[2-5]. We investigated whether JAK
214 inhibitor administration enhanced insulin sensitivity in aged mice. By conducting glucose and
215 insulin tolerance tests, we found that insulin sensitivity was impaired in 22-month- compared to
216 8-month-old mice (Figure 8e). JAK inhibitor improved glucose homeostasis (Figure 8a,b) and
217 insulin sensitivity (Figure 8d,e) in 22-month-old mice, while it had little effect in young mice
218 (Figure 8-figure supplement 1). Glucose-stimulated insulin secretion capacity was not altered by
219 JAK inhibition in 22-month-old mice (Figure 8c), suggesting that pancreatic islet function might
220 not be affected. Fasting glucose was also unchanged with JAK inhibitor treatment (Figure 8e).
221 To test whether insulin sensitivity in fat tissue of aged mice was improved by JAK inhibitor, we
222 performed an *ex vivo* insulin challenge test and found that fat tissue isolated from the JAK
223 inhibitor-treated group exhibited more robust induction of p-AKT in response to insulin

224 compared to the control group (Figure 8g,h). Therefore, it appears that improved fat tissue
225 function through JAK inhibition possibly contributed to enhanced insulin sensitivity in aged
226 mice.

227

228 **Discussion**

229 Adipose tissue is a key metabolic organ, dysfunction of which can be linked to metabolic
230 disease, particularly type 2 diabetes[4]. Adipose tissue function declines with age[5], likely
231 contributing to increased prevalence of metabolic disorders with aging. Thus, potential
232 pharmacotherapies that alleviate age-related adipose tissue dysfunction may lead to important
233 clinical benefit. Previously, we found that senescent cells contribute to age-related adipose tissue
234 dysfunction in a progeroid mouse model[39]. Here, we used progenitor cells isolated from human
235 adipose tissue to demonstrate that senescent cells directly inhibit adipogenesis of non-senescent
236 human fat progenitors. One mechanism by which senescent cells exert this inhibitory effect is
237 through secretion of activin A, a protein that we previously showed inhibits adipogenesis[43]. We
238 tested the role of senescent cells in naturally-aged INK-ATTAC mice and confirmed that
239 senescent cells play a causal role in age-related fat dysfunction *in vivo*. Moreover, we found that
240 JAK inhibitor reduced activin A secretion both *in vitro* and *in vivo*. Two months of JAK inhibitor
241 administration preserved adipose tissue function and restored insulin sensitivity in 22-month-old
242 mice. Our study provides proof-of-concept evidence that senescent cells play an important role in
243 age-related adipose tissue loss and dysfunction. It also suggests that inhibiting the JAK signaling
244 pathway or selectively eliminating senescent cells hold promise as avenues to prevent or treat
245 age-related metabolic dysfunction.

246 The JAK/STAT pathway plays an important role in adipose tissue development and
247 function[48]. Previously, we found that JAK inhibitor treatment inhibited production of SASP
248 factors and improved physical function in aged mice [31]. Here, we show that JAK1/2 inhibition
249 has metabolic benefits in aged mice. JAK inhibitor treatment suppressed activin A production by
250 senescent cells *in vitro* and in fat progenitors, fat tissue, and the circulation in aged mice. These

251 observations are concordant with improved adipogenesis and reduced activin A in fat tissue after
252 genetic clearance of senescent cells from 18-month-old INK-ATTAC$^{+/-}$ mice. One possible
253 mechanism for improved adipogenesis and fat tissue function by JAK inhibitor treatment is
254 reduction of activin A production by senescent cells. Other SASP components (i.e. IL-6, TNFα,
255 and IFNγ) may also contribute to impairment of adipose tissue function in aged animals.

256 It is possible that mechanisms other than those directly affecting senescent cells
257 contributed to the improved adipogenesis we found. Also, senescent cells of many types and in
258 multiple tissues, not only in fat, are likely affected by systemic administration of JAK1/2
259 inhibitors to mice or AP20187 to INK-ATTAC animals. Very likely, these systemic effects of
260 our interventions contributed to alleviating metabolic dysfunction. To partially address this,
261 rather than conducting an epistasis experiment (treating senescent cell-depleted INK-ATTAC
262 mice with JAK inhibitor to check for off-target effects), we compared effects of JAK inhibitor
263 treatment in old to young mice, since the latter have fewer senescent cells, like AP20187-treated
264 INK-ATTAC mice. We feel this experiment achieves essentially the same goals as would an
265 epistasis experiment, and arguably may even have certain advantages: potential off-target effects
266 of AP20187 are avoided and senescent cells are very few in young mice, unlike older AP20187-
267 treated INK-ATTAC mice, in which more than 50% of senescent cells can remain after treatment
268 with AP20187 (Figure 4-figure supplement 1). The lack of substantial effects of JAK inhibitor
269 treatment on adipogenesis, fat depot weights, and insulin sensitivity in young animals, but strong
270 effects in old animals with higher senescent cell burden and activin A, coupled with parallel
271 effects between JAK inhibitor treatment in wild type mice to those of genetic clearance with
272 AP20187 in INK-ATTAC mice, suggest that effects of JAK inhibitors on senescent cells may
273 contribute to improved metabolic function in older mice.

274 Our findings are consistent with the speculation that impaired adipogenesis leads to
275 ectopic lipid accumulation and insulin resistance[4]. We found that JAK pathway inhibition led to
276 maintained fat mass and enhanced metabolic function in tandem with improved adipogenic
277 capacity in aged mice. Expression of *PPARγ* and *C/EBPα*, both of which are essential for insulin
278 sensitivity[9,49], increased in adipose tissue of JAK inhibitor-treated mice. These changes were
279 accompanied by reduced circulating FFAs and hepatic lipid accumulation, two important
280 manifestations of lipotoxicity associated with insulin resistance[14,50]. Indeed, JAK inhibition
281 improved insulin sensitivity in these mice. In addition to improved adipogenesis, JAK inhibition
282 reduces systemic inflammation (including reducing circulating IL6) in aged mice[31] and promotes
283 "browning" of adipose tissue[51], both of which are known to affect adipogenesis and insulin
284 sensitivity. These mechanisms might also contribute to improved insulin sensitivity in aged mice
285 in addition to reduced activin A level. Importantly, JAK inhibition improved adipogenesis and
286 insulin sensitivity in aged mice but did so much less in younger mice, suggesting that the JAK
287 pathway participates in age- or senescence-related pathogenesis of adipose tissue dysfunction.
288 Furthermore, the effects of JAK inhibitors seem to be similar in mouse, rat, and human models.
289 This is consistent with the speculation that the most fundamental aging mechanisms are
290 conserved across mammalian species.

291 Activin A is a member of the transforming growth factor superfamily and is involved in a
292 variety of biological events[52]. Activin A has widespread effects on multiple types of
293 progenitors[43,53] both directly and through interaction with the closely related growth and
294 differentiation factors (GDFs), which share receptor and signaling mechanisms with activin A[54].
295 Our results suggest that circulating activin A levels could be a bio-marker of senescent cell
296 burden since: 1) circulating levels of activin A increase with aging, consistent with the increase

297 in senescent cell abundance with aging, 2) senescent cells secrete activin A, 3) genetic clearance
298 of senescent cells from 18-month-old INK-ATTAC$^{+/-}$ mice reduced circulating activin A, and 4)
299 JAK inhibition suppresses activin A production in senescent cells *in vitro* and in aged mice *in*
300 *vivo*. It is important to note that a variety of cell types can regulate activin A production,
301 including macrophages[43]. It is possible that these cell types contribute to increased activin A
302 levels with aging. It will be valuable to study the effect of specific inhibition of activin A during
303 aging. However, most activin A-blocking agents such as follistatin also inhibit myostatin due to
304 structural similarity to activin A[55,56]. These agents would therefore be anticipated to alter both
305 muscle and fat mass though additional mechanisms that may be independent of activin A[57,58].

306 JAK inhibitor treatment did not alter lean mass in aged mice (Figure 6b,e). Thus, JAK
307 inhibition might be superior to current activin A-blocking agents for alleviation of age-related
308 adipose tissue dysfunction. Ruxolitinib, the JAK1/2 inhibitor we used *in vivo*, is approved by
309 FDA for treating myelofibrosis[59-61]. Although it has side-effects in human subjects with
310 myelofibrosis including anemia and thrombocytopenia[59,61], we and others found that ruxolitinib
311 has minimal effects on peripheral blood cell populations in both young [62] and old mice[31].
312 Considerable work remains to be done to assess potential side-effects from JAK1/2 inhibitors,
313 especially in older subjects. We stress this needs to be done before contemplating their use for
314 age-related dysfunction in clinical practice.

315 We observed an unusually rapid loss of fat from 18-month old INK-ATTAC$^{+/-}$ mice
316 within 3 weeks. This fat loss could be related to the need to administer AP20187 by
317 intraperitoneal (ip) injection, despite our making every effort to reduce this effect. Both WT and
318 INK-ATTAC$^{+/-}$ mice were injected ip with AP20187 for three consecutive days, with 14 days
319 between treatments. Thus, both groups received 6 ip injections within 3 weeks, the stress from

320 which might have accelerated fat loss. Due to limited numbers of naturally aged INK-ATTAC$^{+/-}$
321 mice, we selected the most closely matched control group to detect an effect of clearing
322 senescent cells on activin A and adipogenesis. The strategy of treating both the WT and INK-
323 ATTAC$^{+/-}$ littermates with AP20187 had the advantages that both the treated and control groups
324 received ip injection of the same drug in parallel. We used 18-month-old INK-ATTAC$^{+/-}$ mice
325 because we have previously observed that 18 month old mice already have a detectable increase
326 in senescent cell burden in their adipose tissue[32]. In addition, we decided to focus on the acute
327 effect of clearance of senescent cells from INK-ATTAC$^{+/-}$ mice on adipogenic transcription
328 factor expression, which can precede other changes. Therefore, we decided to treat these INK-
329 ATTAC$^{+/-}$ mice for 3 weeks. Intermittent clearance of senescent cells with AP20187 was used
330 based on our recent finding that senolytics are effective when administered intermittently, likely
331 because senescent cells do not divide and may be slow to re-accumulate once cleared in the
332 absence of a strong continuing insult[63]. Furthermore, AP20187 has to be administered i.p.,
333 precluding daily administration. On the other hand, we showed that JAK inhibitors, which blunt
334 the SASP and can be administered orally, need to be continuously present to inhibit the SASP[31].

335 In summary, we demonstrated a likely causal role for senescent cells in age-related fat
336 dysfunction and discovered a novel mechanism through which senescent cells can directly impair
337 healthy fat progenitor function. Pharmacologic inhibition of the JAK pathway reduced activin A
338 production *in vitro* and *in vivo*, alleviated age-related adipose tissue dysfunction, and improved
339 insulin sensitivity in aged mice. Albeit speculative, our findings are consistent with the general
340 hypothesis that senescent cells might exert profound effects on tissue and organismal function by
341 affecting normal progenitors or stem cells through production of TGFβ family members, such as
342 activin A, and potentially other types of factors secreted by senescent cells. Our work suggests

343 that targeting senescent cells or their products could be a promising avenue for delaying,
344 preventing, alleviating, or treating age-related stem cell, progenitor, and adipose tissue
345 dysfunction and metabolic disease.

346

347 **Materials and Methods**

348 **Cell Culture and Reagents**

349 Primary human fat progenitors were isolated from subcutaneous fat collected from
350 healthy, lean (BMI 26.6±0.9 kg/m^2) kidney donors aged 39±3.3 years as previously described[64].
351 The protocol (10-005236) was approved by the Mayo Clinic Foundation Institutional Review
352 Board for Human Research. Informed consent and consent to publish was obtained from all
353 human subjects. Rat fat progenitors were isolated from 3- and 30-month-old Brown Norway rats
354 (purchased from Harlan Sprague Dawley) as previously described[26]. All rat and mouse
355 experimental procedures (A21013, A37715 and A16315) were approved by the Institutional
356 Animal Care and Use Committee (IACUC) at Mayo Clinic. Human fat cell progenitors were
357 subjected to 10 Gy of cesium radiation to induce senescence as described previously[31]. Human
358 fat cell progenitors were also treated with 0.2μM doxorubicin for 24 hours to induce senescence.
359 Senescence was induced by irradiation unless otherwise indicated. For co-culture experiments,
360 primary progenitors were stained with CellTracker CM-DiI dye (Thermo Fisher Scientific,
361 Waltham, MA, USA) according to the manufacturer's instructions. These cells were then seeded
362 into wells containing either non-senescent control or senescent progenitors. The mixtures of cells
363 were differentiated for 15 days. Differentiation of progenitors was assessed by observers who
364 were not aware of which treatments the cultures had been exposed to. Cells with multiple
365 doubly-refractile lipid inclusions visible by low power phase contrast microscopy were
366 considered to be differentiated[44].

367 JAK inhibitor 1 (CAS 457081-03-7) was purchased from EMD Millipore (Billerica, MA,
368 USA). Ruxolitinib (INCB18424, CAS 941678-49-5) was purchased from ChemieTek
369 (Indianapolis, IN, USA). Amicon Ultra centrifugal filters were purchased from EMD Millipore.

370 Activin A ELISA kits (catalog number: DAC00B) and activin A neutralizating antibody (catalog
371 number: MAB3381) were purchased from R&D Systems (Minneapolis, MN, USA). SB 431542
372 was purchased from Cayman Chemical (Ann Arbor, MI, USA).

373 **Conditioned Medium Collection**

374 Cells were washed with PBS 3 times and cultured in medium to be conditioned (CM)
375 containing 1 mM sodium pyruvate, 2 mM glutamine, MEM vitamins, MEM non-essential amino
376 acids, and antibiotic (Thermo Fisher Scientific) for 24 hours. For JAK inhibitor treatment, cells
377 were treated with 0.6μM JAK inhibitor or DMSO for 48 hours in regular medium, washed with
378 PBS 3 times, and then exposed to CM containing JAK inhibitor or DMSO for another 24 hours.

379 **Fat Progenitor Differentiation**

380 For differentiation, confluent human primary progenitors were treated with differentiation
381 medium (DM) containing DMEM/F12, 15nM HEPES, 15mM $NaHCO_3$, 2mM glutamine,
382 10mg/L transferrin, 33μM biotin, 0.5μM insulin, 17μM pantothenate, 0.1μM dexamethasone,
383 2nM triiodo-L-thyronine (T3), 540μM 3-isobutyl-1-methylxanthine (IBMX), 1μM ciglitazone,
384 1mg/ml fetuin, and penicillin/streptomycin for 15 days unless indicated otherwise. For
385 conditioned medium experiments, 2x-DM was prepared by doubling the concentration of key
386 differentiation ingredients (20mg/L transferrin, 66μM biotin, 1μM insulin, 34μM pantothenate,
387 0.2μM dexamethasone, 4nM T3, 1080 μM IBMX, 2μM ciglitazone, and 2mg/ml fetuin). Pooled
388 cells isolated from several human subjects were then differentiated with CM mixed with 2x-DM
389 at a 1:1 ratio for 15 days unless indicated otherwise. The media were changed every 2 days. To
390 induce differentiation of rat cells, confluent fat progenitors were exposed to DM containing 5
391 μg/ml insulin, 10 μg/ml transferrin, and 0.2nM triiodothyronine in DMEM/F-12 for 48 hours.

392 DMEM/F12 and glutamine were purchased from Thermo Fisher Scientific. All other reagents
393 were purchased from Sigma-Aldrich (St. Louis, MO, USA).

394 **Real-Time PCR**

395 Trizol (Thermo Fisher Scientific) was used to extract RNA from tissues or cells. M-MLV
396 Reverse Transcriptase kit (Thermo Fisher Scientific) was used for reverse transcription. Real-
397 time PCR was performed using TaqMan fast advanced master mix. All reagents including probes
398 and primers were purchased from Thermo Fisher Scientific. TATA-binding protein (TBP) was
399 used as an internal control.

400 **Western Blotting**

401 Cells or tissues were homogenized in cell lysis buffer (Cell Signaling, Danvers, MA,
402 USA) with protease inhibitors (Sigma-Aldrich). Coumassie Plus reagents (Pierce, Rockford, IL,
403 USA) were used to determine total protein content. Proteins were loaded on SDS-PAGE gels and
404 transferred to immuno-blot PVDF membranes (Biorad, Hercules, CA, USA). SuperSignal West
405 Pico Chemiluminescent Substrate (Pierce) was used to develop signals. p-AKT (#4060) and
406 total-AKT (#4691) antibodies were purchased from Cell Signaling.

407 **Comprehensive Laboratory Animal Monitoring System and SABG activity assay**

408 Metabolic rate and food intake were measured using a Comprehensive Laboratory
409 Animal Monitoring System (CLAMS) as previously described[31]. Adipose tissue cellular SABG
410 was assayed as previously described[31]. $SABG^+$ cells were quantified by observers who were not
411 aware of which treatments cultures had been exposed to.

412 **Mice and Drug Treatments**

413 Experimental procedures (A21013, A37715 and A16315) were approved by the IACUC
414 at Mayo Clinic. Twenty two-month-old C57BL/6 male mice were obtained from the National
415 Institute on Aging (NIA). INK-ATTAC$^{+/-}$ transgenic mice were generated and genotyped as
416 previously described[39]. Mice were maintained under a 12 hour light and 12 hour dark cycle at
417 24°C with free access to food (standard mouse diet, Lab Diet 5053, St. Louis, MO, USA) and
418 water in a pathogen-free facility. For drug treatment, ruxolitinib was dissolved in DMSO and
419 then mixed with food. In addition to regular food, each mouse was fed a small amount of food
420 (0.5g) containing ruxolitinib 60mg/kg (drug/body weight) or DMSO daily. During the treatment,
421 all mice consumed the drug-containing food completely every day. For AP20187 (10mg/kg)
422 treatment, drug was administered by i.p. injection for three consecutive days, with 14 days
423 between treatments. Intermittent clearance of senescent cells with AP20187 was used based on
424 our recent finding that senolytics are effective when administered intermittently[63].

425 **Metabolic Parameter Measurement**

426 For oral glucose tolerance testing, mice were fasted for 6 hours and glucose (2g/kg body
427 weight) was administrated by oral gavage. For insulin tolerance testing, mice were fasted for 4
428 hours and insulin (0.6unit/kg body weight) was injected intraperitoneally. Glucose was measured
429 using a handheld glucometer (Bayer) in blood from the tail vein. For the glucose-stimulated
430 insulin secretion assay, mice were fasted for 6 hours and glucose (2g/kg body weight) was
431 administrated by oral gavage. Blood samples were collected at baseline, 20 minutes, and 60
432 minutes after glucose administration. Plasma insulin levels were measured by ELISA (ALPCO,
433 Salem, NH, USA). Fat and lean mass were measured by MRI (Echo Medical Systems, Houston,
434 TX, USA). Hepatic TG was measured as previously described[65]. FFA and TG were measured
435 using kits from Wako Chemicals (Richmond, VA, USA). In all studies, investigators conducting

436 analyses of animals were not aware of which treatments animals had received.

437 **Statistical Methods**

438 Two-tailed Student's t tests were used to determine statistical significance. $p<0.05$ was
439 considered significant. All values are expressed as mean ± s.e.m. No randomization was used to
440 assign experimental groups. We determined the sample size based on our previous experiments,
441 so no statistical power analysis was used. All replicates in this study were independent biological
442 replicates, which came from different biological samples.

443

444 **Acknowledgements**

445 The authors are grateful to C. Guo for helping with ruxolitinib administration, J. Armstrong for
446 administrative assistance, and M. Mahlman for obtaining human fat samples. This work was
447 supported by NIH grants AG13925 (JLK), AG041122 (JLK), AG31736 (Project 4: JLK),
448 AG044396 (JLK), DK50456 (JLK), AG46061 (AKP), the Connor Group, and the Glenn, Ted
449 Nash Long Life, and Noaber Foundations (JLK). MX received a Glenn/American Federation for
450 Aging Research Postdoctoral Fellowship for Translational Research on Aging.

451

452 **Author Contributions**

453 MX, TT, and JLK conceived the project and designed the experiments. MX, AKP, TT, TP, HD,
454 TAW, KOJ, and MBS performed animal studies. MX and MMW performed cell culture studies.
455 NG and MDJ contributed to isolation of primary human preadipocytes. MX, AKP, HD, MMW,
456 and TAW analyzed the data. MDJ and NKL contributed to manuscript preparation. MX, AKP,
457 TT, and JLK wrote the manuscript. JLK and TT oversaw all experimental design, data analysis,
458 and manuscript preparation. All authors revised and approved the manuscript.

459 **References**

460 1 Listenberger, L. L. *et al.* Triglyceride accumulation protects against fatty acid-induced
461 lipotoxicity. *Proceedings of the National Academy of Sciences of the United States of*
462 *America* **100**, 3077-3082, doi:10.1073/pnas.0630588100 (2003).
463 2 Wang, M. Y. *et al.* Adipogenic capacity and the susceptibility to type 2 diabetes and
464 metabolic syndrome. *Proceedings of the National Academy of Sciences of the United*
465 *States of America* **105**, 6139-6144, doi:10.1073/pnas.0801981105 (2008).
466 3 Unger, R. H. & Scherer, P. E. Gluttony, sloth and the metabolic syndrome: a roadmap to
467 lipotoxicity. *Trends in endocrinology and metabolism: TEM* **21**, 345-352,
468 doi:10.1016/j.tem.2010.01.009 (2010).
469 4 Gustafson, B., Hedjazifar, S., Gogg, S., Hammarstedt, A. & Smith, U. Insulin resistance
470 and impaired adipogenesis. *Trends in endocrinology and metabolism: TEM* **26**, 193-200,
471 doi:10.1016/j.tem.2015.01.006 (2015).
472 5 Tchkonia, T. *et al.* Fat tissue, aging, and cellular senescence. *Aging Cell* **9**, 667-684,
473 doi:10.1111/j.1474-9726.2010.00608.x (2010).
474 6 Tchkonia, T. *et al.* Mechanisms and metabolic implications of regional differences
475 among fat depots. *Cell Metab* **17**, 644-656, doi:10.1016/j.cmet.2013.03.008 (2013).
476 7 Spalding, K. L. *et al.* Dynamics of fat cell turnover in humans. *Nature* **453**, 783-787,
477 doi:10.1038/nature06902 (2008).
478 8 Tchoukalova, Y. D. *et al.* Regional differences in cellular mechanisms of adipose tissue
479 gain with overfeeding. *Proceedings of the National Academy of Sciences of the United*
480 *States of America* **107**, 18226-18231, doi:10.1073/pnas.1005259107 (2010).
481 9 Wu, Z. *et al.* Cross-regulation of C/EBP alpha and PPAR gamma controls the
482 transcriptional pathway of adipogenesis and insulin sensitivity. *Molecular cell* **3**, 151-158
483 (1999).
484 10 Lin, F. T. & Lane, M. D. CCAAT/enhancer binding protein alpha is sufficient to initiate
485 the 3T3-L1 adipocyte differentiation program. *Proceedings of the National Academy of*
486 *Sciences of the United States of America* **91**, 8757-8761 (1994).
487 11 Bernlohr, D. A., Simpson, M. A., Hertzel, A. V. & Banaszak, L. J. Intracellular lipid-
488 binding proteins and their genes. *Annual review of nutrition* **17**, 277-303,
489 doi:10.1146/annurev.nutr.17.1.277 (1997).
490 12 Sun, Z. *et al.* Perilipin1 promotes unilocular lipid droplet formation through the
491 activation of Fsp27 in adipocytes. *Nature communications* **4**, 1594,
492 doi:10.1038/ncomms2581 (2013).
493 13 Garbarino, J. & Sturley, S. L. Saturated with fat: new perspectives on lipotoxicity.
494 *Current opinion in clinical nutrition and metabolic care* **12**, 110-116,
495 doi:10.1097/MCO.0b013e32832182ee (2009).
496 14 Slawik, M. & Vidal-Puig, A. J. Lipotoxicity, overnutrition and energy metabolism in
497 aging. *Ageing Res Rev* **5**, 144-164, doi:10.1016/j.arr.2006.03.004 (2006).
498 15 Tchkonia, T., Corkey, B. & Kirkland, J. in *Overweight and the Metabolic Syndrome* Vol.
499 26 *Endocrine Updates* (eds GeorgeA Bray & DonnaH Ryan) Ch. 6, 105-123 (Springer
500 US, 2006).
501 16 Guo, W. *et al.* Aging results in paradoxical susceptibility of fat cell progenitors to
502 lipotoxicity. *Am J Physiol Endocrinol Metab* **292**, E1041-1051,
503 doi:10.1152/ajpendo.00557.2006 (2007).

504 17 Fink, R. I., Kolterman, O. G., Griffin, J. & Olefsky, J. M. Mechanisms of insulin
505 resistance in aging. *The Journal of clinical investigation* **71**, 1523-1535 (1983).
506 18 Tchkonia, T., Zhu, Y., van Deursen, J., Campisi, J. & Kirkland, J. L. Cellular senescence
507 and the senescent secretory phenotype: therapeutic opportunities. *The Journal of clinical*
508 *investigation* **123**, 966-972 (2013).
509 19 Cowie, C. C. *et al.* Prevalence of diabetes and impaired fasting glucose in adults in the
510 U.S. population: National Health And Nutrition Examination Survey 1999-2002.
511 *Diabetes care* **29**, 1263-1268, doi:10.2337/dc06-0062 (2006).
512 20 North, B. J. & Sinclair, D. A. The intersection between aging and cardiovascular disease.
513 *Circulation research* **110**, 1097-1108, doi:10.1161/CIRCRESAHA.111.246876 (2012).
514 21 Palmer, A. K. *et al.* Cellular Senescence in Type 2 Diabetes: A Therapeutic Opportunity.
515 *Diabetes* **64**, 2289-2298, doi:10.2337/db14-1820 (2015).
516 22 Cartwright, M. J., Tchkonia, T. & Kirkland, J. L. Aging in adipocytes: potential impact of
517 inherent, depot-specific mechanisms. *Exp Gerontol* **42**, 463-471,
518 doi:10.1016/j.exger.2007.03.003 (2007).
519 23 Raguso, C. A. *et al.* A 3-year longitudinal study on body composition changes in the
520 elderly: role of physical exercise. *Clinical nutrition* **25**, 573-580,
521 doi:10.1016/j.clnu.2005.10.013 (2006).
522 24 Kuk, J. L., Saunders, T. J., Davidson, L. E. & Ross, R. Age-related changes in total and
523 regional fat distribution. *Ageing Res Rev* **8**, 339-348, doi:10.1016/j.arr.2009.06.001
524 (2009).
525 25 Cartwright, M. J. *et al.* Aging, depot origin, and preadipocyte gene expression. *J*
526 *Gerontol A Biol Sci Med Sci* **65**, 242-251, doi:10.1093/gerona/glp213 (2010).
527 26 Tchkonia, T. *et al.* Increased TNFalpha and CCAAT/enhancer-binding protein
528 homologous protein with aging predispose preadipocytes to resist adipogenesis. *Am J*
529 *Physiol Endocrinol Metab* **293**, E1810-1819, doi:10.1152/ajpendo.00295.2007 (2007).
530 27 Karagiannides, I. *et al.* Altered expression of C/EBP family members results in decreased
531 adipogenesis with aging. *Am J Physiol Regul Integr Comp Physiol* **280**, R1772-1780
532 (2001).
533 28 Kirkland, J. L., Hollenberg, C. H. & Gillon, W. S. Age, anatomic site, and the replication
534 and differentiation of adipocyte precursors. *Am J Physiol* **258**, C206-210 (1990).
535 29 Hayflick, L. & Moorhead, P. S. The serial cultivation of human diploid cell strains.
536 *Experimental cell research* **25**, 585-621 (1961).
537 30 Campisi, J. & d'Adda di Fagagna, F. Cellular senescence: when bad things happen to
538 good cells. *Nat Rev Mol Cell Biol* **8**, 729-740 (2007).
539 31 Xu, M. *et al.* JAK inhibition alleviates the cellular senescence-associated secretory
540 phenotype and frailty in old age. *Proceedings of the National Academy of Sciences*,
541 doi:10.1073/pnas.1515386112 (2015).
542 32 Stout, M. B. *et al.* Growth hormone action predicts age-related white adipose tissue
543 dysfunction and senescent cell burden in mice. *Aging (Albany NY)* **6**, 575-586 (2014).
544 33 Coppe, J. P. *et al.* Senescence-associated secretory phenotypes reveal cell-
545 nonautonomous functions of oncogenic RAS and the p53 tumor suppressor. *PLoS Biol* **6**,
546 2853-2868, doi:10.1371/journal.pbio.0060301 (2008).
547 34 Coppe, J. P. *et al.* A human-like senescence-associated secretory phenotype is conserved
548 in mouse cells dependent on physiological oxygen. *PLoS One* **5**, e9188 (2010).

549 35 Park, J. S. *et al.* Increased caveolin-1, a cause for the declined adipogenic potential of
550 senescent human mesenchymal stem cells. *Mech Ageing Dev* **126**, 551-559,
551 doi:10.1016/j.mad.2004.11.014 (2005).
552 36 Mitterberger, M. C., Lechner, S., Mattesich, M. & Zwerschke, W. Adipogenic
553 differentiation is impaired in replicative senescent human subcutaneous adipose-derived
554 stromal/progenitor cells. *J Gerontol A Biol Sci Med Sci* **69**, 13-24,
555 doi:10.1093/gerona/glt043 (2014).
556 37 Acosta, J. C. *et al.* A complex secretory program orchestrated by the inflammasome
557 controls paracrine senescence. *Nature cell biology* **15**, 978-990, doi:10.1038/ncb2784
558 (2013).
559 38 Nelson, G. *et al.* A senescent cell bystander effect: senescence-induced senescence.
560 *Aging Cell* **11**, 345-349, doi:10.1111/j.1474-9726.2012.00795.x (2012).
561 39 Baker, D. J. *et al.* Clearance of p16Ink4a-positive senescent cells delays ageing-
562 associated disorders. *Nature* **479**, 232-236 (2011).
563 40 Gustafson, B. & Smith, U. Cytokines promote Wnt signaling and inflammation and
564 impair the normal differentiation and lipid accumulation in 3T3-L1 preadipocytes. *The*
565 *Journal of biological chemistry* **281**, 9507-9516, doi:10.1074/jbc.M512077200 (2006).
566 41 Okada, A. *et al.* Adipogenesis of the mesenchymal stromal cells and bone oedema in
567 rheumatoid arthritis. *Clin Exp Rheumatol* **30**, 332-337 (2012).
568 42 McGillicuddy, F. C. *et al.* Interferon gamma attenuates insulin signaling, lipid storage,
569 and differentiation in human adipocytes via activation of the JAK/STAT pathway. *The*
570 *Journal of biological chemistry* **284**, 31936-31944, doi:10.1074/jbc.M109.061655 (2009).
571 43 Zaragosi, L. E. *et al.* Activin a plays a critical role in proliferation and differentiation of
572 human adipose progenitors. *Diabetes* **59**, 2513-2521, doi:10.2337/db10-0013 (2010).
573 44 Karagiannides, I. *et al.* Increased CUG triplet repeat-binding protein-1 predisposes to
574 impaired adipogenesis with aging. *The Journal of biological chemistry* **281**, 23025-23033,
575 doi:10.1074/jbc.M513187200 (2006).
576 45 Inman, G. J. *et al.* SB-431542 is a potent and specific inhibitor of transforming growth
577 factor-beta superfamily type I activin receptor-like kinase (ALK) receptors ALK4, ALK5,
578 and ALK7. *Molecular pharmacology* **62**, 65-74 (2002).
579 46 Nadra, K. *et al.* Cell autonomous lipin 1 function is essential for development and
580 maintenance of white and brown adipose tissue. *Molecular and cellular biology* **32**,
581 4794-4810, doi:10.1128/MCB.00512-12 (2012).
582 47 Donkor, J., Sparks, L. M., Xie, H., Smith, S. R. & Reue, K. Adipose tissue lipin-1
583 expression is correlated with peroxisome proliferator-activated receptor alpha gene
584 expression and insulin sensitivity in healthy young men. *J Clin Endocrinol Metab* **93**,
585 233-239, doi:10.1210/jc.2007-1535 (2008).
586 48 Richard, A. J. & Stephens, J. M. The role of JAK-STAT signaling in adipose tissue
587 function. *Biochim Biophys Acta* **1842**, 431-439, doi:10.1016/j.bbadis.2013.05.030 (2014).
588 49 El-Jack, A. K., Hamm, J. K., Pilch, P. F. & Farmer, S. R. Reconstitution of insulin-
589 sensitive glucose transport in fibroblasts requires expression of both PPARgamma and
590 C/EBPalpha. *The Journal of biological chemistry* **274**, 7946-7951 (1999).
591 50 Boden, G. Obesity, insulin resistance and free fatty acids. *Current opinion in*
592 *endocrinology, diabetes, and obesity* **18**, 139-143, doi:10.1097/MED.0b013e3283444b09
593 (2011).

51 Moisan, A. *et al.* White-to-brown metabolic conversion of human adipocytes by JAK inhibition. *Nature cell biology* **17**, 57-67, doi:10.1038/ncb3075 (2015).
52 Xia, Y. & Schneyer, A. L. The biology of activin: recent advances in structure, regulation and function. *J Endocrinol* **202**, 1-12, doi:10.1677/JOE-08-0549 (2009).
53 Bowser, M. *et al.* Effects of the activin A-myostatin-follistatin system on aging bone and muscle progenitor cells. *Exp Gerontol* **48**, 290-297, doi:10.1016/j.exger.2012.11.004 (2013).
54 Sako, D. *et al.* Characterization of the ligand binding functionality of the extracellular domain of activin receptor type IIb. *The Journal of biological chemistry* **285**, 21037-21048, doi:10.1074/jbc.M110.114959 (2010).
55 Cash, J. N., Rejon, C. A., McPherron, A. C., Bernard, D. J. & Thompson, T. B. The structure of myostatin:follistatin 288: insights into receptor utilization and heparin binding. *Embo J* **28**, 2662-2676, doi:10.1038/emboj.2009.205 (2009).
56 Nakatani, M. *et al.* Transgenic expression of a myostatin inhibitor derived from follistatin increases skeletal muscle mass and ameliorates dystrophic pathology in mdx mice. *Faseb J* **22**, 477-487, doi:10.1096/fj.07-8673com (2008).
57 Lee, S. J. Regulation of muscle mass by myostatin. *Annual review of cell and developmental biology* **20**, 61-86, doi:10.1146/annurev.cellbio.20.012103.135836 (2004).
58 McPherron, A. C. & Lee, S. J. Suppression of body fat accumulation in myostatin-deficient mice. *The Journal of clinical investigation* **109**, 595-601, doi:10.1172/JCI13562 (2002).
59 Verstovsek, S. *et al.* Safety and efficacy of INCB018424, a JAK1 and JAK2 inhibitor, in myelofibrosis. *The New England journal of medicine* **363**, 1117-1127, doi:10.1056/NEJMoa1002028 (2010).
60 Harrison, C. *et al.* JAK inhibition with ruxolitinib versus best available therapy for myelofibrosis. *N Engl J Med* **366**, 787-798, doi:10.1056/NEJMoa1110556 (2012).
61 Verstovsek, S. *et al.* A double-blind, placebo-controlled trial of ruxolitinib for myelofibrosis. *The New England journal of medicine* **366**, 799-807, doi:10.1056/NEJMoa1110557 (2012).
62 Quintas-Cardama, A. *et al.* Preclinical characterization of the selective JAK1/2 inhibitor INCB018424: therapeutic implications for the treatment of myeloproliferative neoplasms. *Blood* **115**, 3109-3117 (2010).
63 Zhu, Y. *et al.* The Achilles' heel of senescent cells: from transcriptome to senolytic drugs. *Aging Cell*, doi:10.1111/acel.12344 (2015).
64 Tchkonia, T. *et al.* Abundance of two human preadipocyte subtypes with distinct capacities for replication, adipogenesis, and apoptosis varies among fat depots. *Am J Physiol Endocrinol Metab* **288**, E267-277, doi:10.1152/ajpendo.00265.2004 (2005).
65 Xu, M. *et al.* Ncb5or deficiency increases fatty acid catabolism and oxidative stress. *The Journal of biological chemistry* **286**, 11141-11154, doi:10.1074/jbc.M110.196543 (2011).

634 **Figure Titles and Legends**

635 **Figure 1. Adipogenesis in human fat progenitors is impeded by co-culture with senescent**
636 **cells.** Primary subcutaneous human fat progenitors were labelled with DiI and seeded into wells
637 containing either control or radiation-induced senescent preadipocytes. **(a)** Photographs were
638 taken 15 days after initiating differentiation. Representative images are shown. DiI-positive cells
639 are red and DAPI staining is blue. **(b)** Number of differentiated DiI positive cells as a percentage
640 of total DiI positive cells is expressed as mean ± s.e.m. *: $p<0.00001$. Results were obtained
641 using separate strains of fat progenitors harvested from 6 healthy human subjects during surgery
642 to donate a kidney (N=6). Two-tailed Student's t tests were used to determine statistical
643 significance.

644

645 **Figure 2. Conditioned medium from senescent cells impedes adipogenesis in human**
646 **progenitors.** Conditioned medium (CM) was collected from a flask with no cells present (Blank),
647 control non-senescent (CON), and senescent (SEN) fat progenitor cultures. Pooled human
648 progenitors from subcutaneous fat of 5 healthy subjects were treated with 50:50%
649 CM:differentiation medium (DM) for 15 days. **(a)** Representative images are shown at day 5, 10,
650 and 15 of exposure to CM + DM. **(b)** Gene expression was analyzed by real-time PCR at day 5,
651 10, and 15 of exposure to CM + DM. Results are shown as fold change relative to the CON
652 group at day 5. Results were obtained using CM from 5 strains of human primary fat progenitors
653 from different subjects and expressed as mean ± s.e.m. *: $p<0.05$. Two-tailed Student's t tests
654 were used to determine statistical significance.

655 **Figure 3. Inhibition of activin A alleviates the impairment of adipogenesis induced by**
656 **senescent progenitors.** CM was collected from control (CON) and senescent (SEN) fat
657 progenitors. Pooled human progenitors were treated with a 50:50 mixture of CM:DM in the
658 presence of DMSO or 5μM SB431542 (SB431542). **(a)** Representative images are shown of
659 differentiated cells at day 15. **(b)** RNA was collected 7 days after differentiation and real-time
660 PCR was performed. Pooled human progenitors were treated with a 50:50 mixture of CM:DM in
661 the presence or absence of 1μg/ml activin A neutralizing antibody (Activin A AB). **(c)**
662 Representative images are shown of differentiated cells at day 15. **(d)** RNA was collected 7 days
663 after differentiation and real-time PCR was performed. Results are shown as fold change relative
664 to the SEN group. Results were obtained using CM from 5 strains of human primary cells from
665 different subjects and expressed as mean ± s.e.m. *: $p<0.05$. Two-tailed Student's t tests were
666 used to determine statistical significance.

667

668 **Figure 4. Genetic clearance of senescent cells blunts fat loss and increases adipogenic**
669 **markers in fat of 18-month-old mice.** Eighteen-month-old wild-type and INK-ATTAC$^{+/-}$ mice
670 were treated with AP20187 for 3 weeks (10mg/kg, three consecutive days with 14 days rest
671 between treatments; total 6 treatments). Fat mass **(a)** and lean mass **(b)** were measured by MRI
672 along with body weight **(c)** before and after treatment. The percent changes relative to baseline
673 are shown. Results (N=8) are expressed as mean ± s.e.m. *: $p<0.05$ for comparison between WT
674 and INK-ATTAC$^{+/-}$ at 3 weeks. (**d**) SABG^{+} cells were counted in WAT and their percentages as
675 a function of total cells (N=7) are expressed as mean ± s.e.m. *: $p<0.05$. **(e)** Activin A protein in
676 plasma was measured before and after treatment. The percent changes relative to baseline are
677 shown. Results (N=8) are expressed as mean ± s.e.m. *: $p<0.05$ for comparison between WT and

678 INK-ATTAC$^{+/-}$ at 3 weeks. **(f)** RNA from white adipose tissue (WAT) was collected and real-
679 time PCR was performed. Results (N=8) are expressed as mean ± s.e.m. *: p<0.05. Two-tailed
680 Student's t tests were used to determine statistical significance.

681

682 **Figure 5. JAK inhibition suppresses activin A production by senescent fat progenitors and**
683 **partially rescues adipogenesis.** Senescent human progenitors were treated with DMSO (SEN)
684 or 0.6μM JAK inhibitor 1 (SEN+JAKi) for 72 hours. **(a)** RNA was collected from control (CON),
685 SEN, and SEN+JAKi progenitors and real-time PCR was performed. Results (N=7) are
686 expressed as mean ± s.e.m. *: p<0.05. **(b)** CM was collected and activin A protein was assayed
687 by ELISA. Results (N=6) are expressed as mean ± s.e.m. *: p<0.05. **(c)** Representative images
688 are shown of differentiating cells at day 10. **(d)** RNA was collected 10 days after initiation of
689 differentiation and real-time PCR was performed. Results are shown as fold change relative to
690 the SEN group. Results were obtained using CM from 7 strains of human primary progenitors
691 from different subjects and expressed as mean ± s.e.m. *: p<0.05. Two-tailed Student's t tests
692 were used to determine statistical significance.

693

694 **Figure 6. JAK inhibition reduces age-related fat loss in mice.** Twenty-two-month old male
695 mice were treated with vehicle (CON) or ruxolitinib (INCB) for 8 weeks. Fat mass **(a)** and lean
696 mass **(b)** were measured by MRI along with body weight **(c)** before treatment, as well as 1 month
697 and 2 months after treatment. The percent changes relative to baseline are shown for fat mass **(d)**,
698 lean mass **(e)**, and body weight **(f)**. Results (N=9) are expressed as mean ± s.e.m. *: p<0.05.
699 Two-tailed Student's t tests were used to determine statistical significance.

700

701 **Figure 7. JAK inhibition increases adipogenic markers in adipose tissue and decreases**
702 **circulating free fatty acids in aged mice.** Twenty-two-month old male mice were treated with
703 vehicle (CON) or ruxolitinib (INCB) for 8 weeks. **(a)** Weights of different fat depots and liver
704 are shown as percent of whole body weight. Results (N=9) are expressed as mean ± s.e.m. *:
705 p<0.05. **(b)** RNA from WAT was isolated and real-time PCR was performed. Results (N=8) are
706 expressed as mean ± s.e.m. *: p<0.05. **(c)** Plasma activin A protein levels were assayed by
707 ELISA in parallel from 8 six-month-old male mice (Young). Results (N=15 for CON and INCB,
708 N=8 for Young) are expressed as mean ± s.e.m. *: p<0.05. Plasma TG **(d)** and FA **(e)** levels are
709 expressed as mean ± s.e.m. (N=8). *: p<0.05. **(f)** Hepatic TG/protein levels are expressed as
710 mean ± s.e.m. (N=11). **(g)** Total hepatic TG levels are expressed as mean ± s.e.m. (N=11). Two-
711 tailed Student's t tests were used to determine statistical significance.

712

713 **Figure 8. JAK inhibition increases insulin sensitivity in aged mice.** Seven-month old and
714 twenty-two-month old male mice were treated with vehicle (CON) or ruxolitinib (INCB) daily.
715 An oral glucose tolerance test was performed after 5 weeks of treatment. **(a)** Glucose level was
716 monitored over 120 minutes for 22-month old mice (the results for 7-month old mice are shown
717 in Figure 8-figure supplement 1) and **(b)** the area under the curve (AUC) was calculated. Results
718 (N=6 for CON and INCB groups of 8-month-old mice, N=9 for CON and INCB groups of 22-
719 month-old mice) are expressed as mean ± s.e.m. *: p<0.05. **(c)** Plasma insulin was measured at
720 baseline, 20 minutes, and 60 minutes after oral glucose gavage. Results (N=9) are expressed as
721 mean ± s.e.m. *: p<0.05. An insulin tolerance test was performed after 6 weeks of the treatment.
722 **(d)** Glucose was monitored over 120 minutes for 22-month old mice (the results for 7-month old

723 mice are shown in Figure 8-figure supplement 1) and **(e)** area over curve (AOC) was calculated.
724 Results (N=9) are expressed as mean ± s.e.m. *: $p<0.05$. **(f)** Fasting glucose levels (N=9) are
725 expressed as mean ± s.e.m. *: $p<0.05$. **(g)** WAT tissue was collected and cultured in CM with or
726 without 5nM insulin for 5 minutes at 37°C and tissue lysates were then prepared. p-AKT (Ser473)
727 and total AKT protein abundance were assayed. Representative images are shown. **(h)** These
728 signals were quantified by densitometry using ImageJ. The ratios of p-AKT/total AKT are
729 expressed as mean ± s.e.m. N=6. *: $p<0.05$. Two-tailed Student's t tests were used to determine
730 statistical significance.

731

732 **Figure Supplements**

733 **Figure 2-figure supplement 1. Senescent cells impede adipogenesis in fat progenitors.** (**a**)
734 CM was collected from control non-senescent (CON) and senescent (SEN) fat progenitor
735 cultures. Pooled human progenitors from subcutaneous fat of 5 healthy subjects were treated
736 with 50:50% CM:DM for 15 days. Gene expression was analyzed by real-time PCR. Results
737 were obtained using CM from 4 strains of human primary fat progenitors and expressed as mean
738 ± s.e.m. (**b**) Pooled fat progenitors were pre-treated with CM collected from control (CON 24h)
739 and senescent (SEN 24h) cells for 24 hours. Then they were treated with DM for 15 days. Gene
740 expression was analyzed by real-time PCR. Results were obtained from 4 strains of human
741 primary fat progenitors and expressed as mean ± s.e.m. (**c**) CM was collected from non-
742 senescent (CON) and doxorubicin-induced senescent (DOX) fat progenitor cultures. Pooled
743 human progenitors were treated with 50:50% CM:DM for 15 days. Gene expression was
744 analyzed by real-time PCR. Results were obtained using CM from 3 strains of human primary fat
745 progenitors and expressed as mean ± s.e.m. *: $p<0.05$ (**d**) CM was collected from non-senescent
746 (CON) and senescent (SEN) fat progenitor cultures. CM from SEN was separated into two
747 fractions using molecular size filters with a cutoff at ~10kd. The volumes of the fraction larger
748 than ~10kd (>10k) and the fraction smaller than ~10kd (<10k) were matched to CM from SEN
749 using blank CM. Pooled human fat progenitors were treated with 50:50% CM:DM for 10 days.
750 Gene expression was analyzed by real-time PCR. Results were obtained using CM from 3 strains
751 of human primary fat progenitors and expressed as mean ± s.e.m. *: $p<0.05$. **(e)** CM was
752 collected from control non-senescent (CON) and senescent (SEN) fat progenitor cultures. Pooled
753 human progenitors from subcutaneous fat of 5 healthy subjects were treated with 50:50%
754 CM:DM for 5 days in presence of 20μg/ml of IGG (SEN+IGG), IL6 antibody (SEN+IL6 ab),

755 IFNγ antibody (SEN+ IFNγ ab) or TNFα antibody (SEN+TNFα ab). Gene expression was
756 analyzed by real-time PCR. Results were obtained using CM from 2 strains of human primary fat
757 progenitors and expressed as mean ± s.e.m. Two-tailed Student's t tests were used to determine
758 statistical significance.

759

760 **Figure 4-figure supplement 1. Genetic clearance of senescent cells reduced SABG^{+} cells in**
761 **adipose tissue.** Eighteen-month-old wild-type and INK-ATTAC$^{+/-}$ mice were treated with
762 AP20187 for 3 weeks (10mg/kg, three consecutive days with 14 days rest between treatments;
763 total 6 treatments). WAT was collected and assayed for cellular SABG activity and
764 counterstained with DAPI. The SABG^{+} cells are indicated by red arrows.

765

766 **Figure 4-figure supplement 2. Senescent cell clearance blunts fat loss in 18-month INK-**
767 **ATTAC$^{+/-}$ mice.** Eighteen-month-old wild-type and INK-ATTAC$^{+/-}$ mice were treated with
768 AP20187 for 3 weeks (10mg/kg, three consecutive days with 14 days between treatments; total 6
769 treatments). Changes from baseline for fat mass, lean mass, and body weight are shown. Results
770 (N=8) are expressed as mean ± s.e.m. *: $p<0.05$. Two-tailed Student's t tests were used to
771 determine statistical significance.

772

773 **Figure 5-figure supplement 1. Impaired adipogenesis due to effects of senescent cells is**
774 **partially rescued by JAK inhibition.** (**a**) CM was collected from non-senescent (CON) and
775 senescent (SEN) fat progenitor cultures. JAK inhibitor 1(0.6μM) was directly added into CON
776 (CON+JAKi) and SEN (SEN+JAKi) CM. Pooled human fat progenitors were treated with 50:50%

777 CM:DM for 10 days. Gene expression was analyzed by real-time PCR. Results were obtained
778 using CM from 3 strains of human primary fat progenitors and expressed as mean ± s.e.m. (**b**)
779 Rat fat progenitors were isolated from 3 and 30-month old rats. These cells were differentiated in
780 presence of DMSO or 0.6μM JAK inhibitor 1. Representative pictures were shown 48 hours
781 after initiation of differentiation. (**c**) Gene expression was analyzed by real-time PCR in fat
782 progenitors from 30-month old rats. Results (N=4) are expressed as mean ± s.e.m. *: $p<0.05$.
783 Two-tailed Student's t tests were used to determine statistical significance.
784
785 **Figure 6-figure supplement 1. JAK inhibition did not affect metabolic rate or food intake in**
786 **aged mice.** Twenty-two-month old male mice were monitored using CLAMS before and after 8
787 weeks of vehicle (CON) or ruxolitinib (INCB) treatment. **(a)** Metabolic rate and **(b)** food intake
788 (N=7) are expressed as mean ± s.e.m. Two-tailed Student's t tests were used to determine
789 statistical significance.
790
791 **Figure 6-figure supplement 2. JAK inhibition had less impact on body composition and**
792 **adipogenesis in 8-month old mice compared to 22-month old mice.** Eight-month old male
793 mice were treated with vehicle (Y CON) or ruxolitinib (Y INCB) for 8 weeks. (**a**) Fat mass, lean
794 mass, and body weight were measured before and one month after treatment. The percent
795 changes relative to baseline (N=6) are expressed as mean ± s.e.m. (**b**) RNA from WAT was
796 isolated and real-time PCR was performed. Results (N=6) are expressed as mean ± s.e.m. **(c)**
797 WAT was collected from 8-month old (Young) and 22-month old mice (Old). RNA was isolated
798 and real-time PCR was performed. Results (N=6 for Young, N=8 for Old) are expressed as mean
799 ± s.e.m. *: $p<0.05$. Two-tailed Student's t tests were used to determine statistical significance.

800

801 **Figure 7-figure supplement 1. JAK inhibition in aged mice suppressed activin A expression**
802 **in primary fat progenitors.** Twenty-two-month old male mice were treated with vehicle (CON)
803 or ruxolitinib (INCB) for 8 weeks. Fat progenitors were isolated from WAT and gene expression
804 was analyzed by real-time PCR. Some progenitors were pooled from several mice within the
805 same treatment group due to limited yield of cells. Results (N=5 pools, each from different sets
806 of mice) are expressed as mean ± s.e.m. *: $p<0.05$. Two-tailed Student's t tests were used to
807 determine statistical significance.

808

809 **Figure 8-figure supplement 1. JAK inhibition had less impact on glucose tolerance and**
810 **insulin sensitivity in 8-month old mice compared to 22-month old mice.** Eight-month old
811 male mice were treated with vehicle (CON) or ruxolitinib (INCB) for 6 weeks. (**a**) An oral
812 glucose tolerance test was performed after 5 weeks of treatment. Blood glucose was monitored
813 over 120 minutes. Results (N=6) are expressed as mean ± s.e.m. (**b**) An insulin tolerance test was
814 performed after 6 weeks of the treatment. Blood glucose was monitored over 120 minutes.
815 Results (N=6) are expressed as mean ± s.e.m. Two-tailed Student's t tests were used to determine
816 statistical significance.

817

818 **Source Data Files**

819 **Figure 1-source data 1:** Adipogenesis in human fat progenitors is impeded by co-culture with
820 senescent cells.

821 **Figure 2-source data 1:** Conditioned medium from senescent cells impedes adipogenesis in
822 human progenitors.

823 **Figure 3-source data 1:** Inhibition of activin A alleviates the impairment of adipogenesis
824 induced by senescent progenitors.

825 **Figure 4-source data 1:** Genetic clearance of senescent cells blunts fat loss and increases
826 adipogenic markers in fat of 18-month-old mice.

827 **Figure 5-source data 1:** JAK inhibition suppresses activin A production by senescent fat
828 progenitors and partially rescues adipogenesis.

829 **Figure 6-source data 1:** JAK inhibition reduces age-related fat loss in mice.

830 **Figure 7-source data 1:** JAK inhibition increases adipogenic markers in adipose tissue and
831 decreases circulating free fatty acids in aged mice.

832 **Figure 8-source data 1:** JAK inhibition increases insulin sensitivity in aged mice.

833

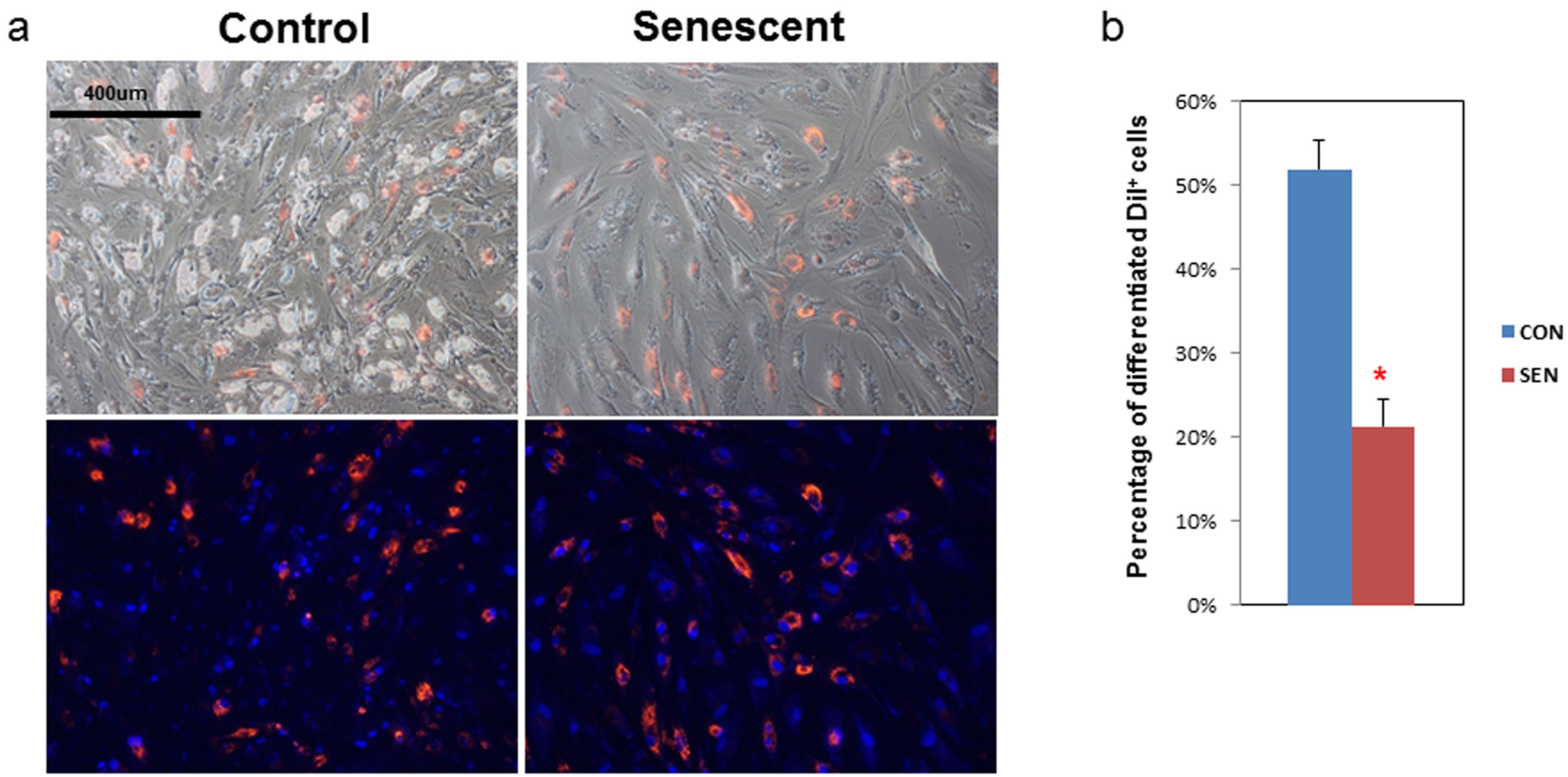
a
Control
Senescent
400um
b
Percentage of differentiated DiI+ cells
60%
50%
40%
30%
20%
10%
0%
*
CON
SEN

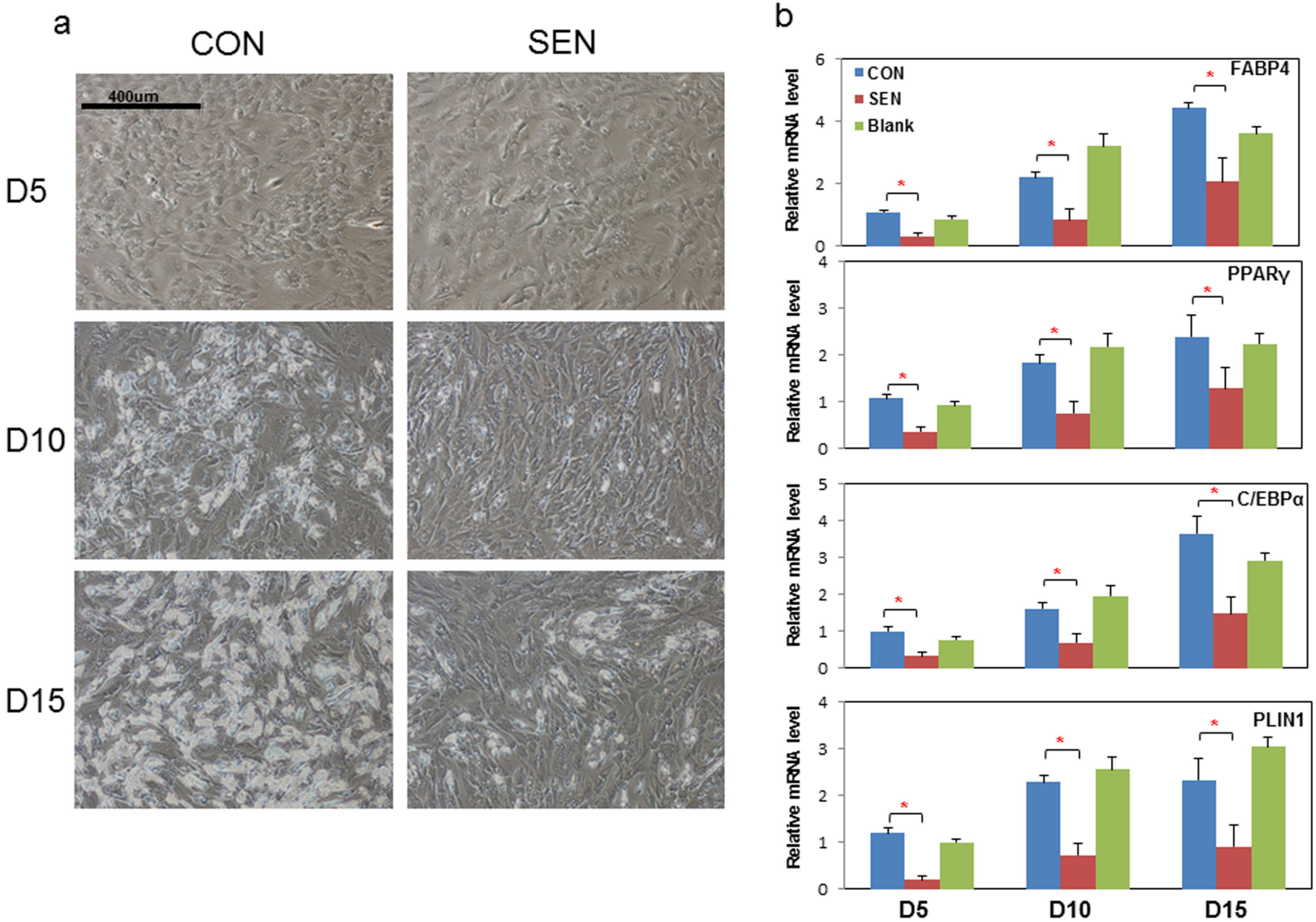
a
CON
SEN
400um
D5
D10
D15
b
CON
SEN
Blank
FABP4
PPARγ
C/EBPα
PLIN1
Relative mRNA level
D5
D10
D15

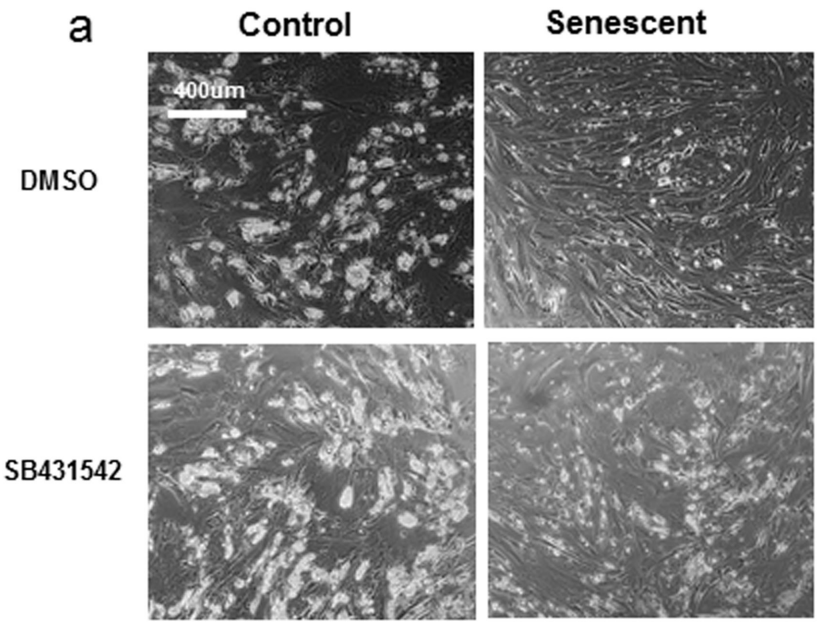
a
Control
Senescent
400um
DMSO
SB431542

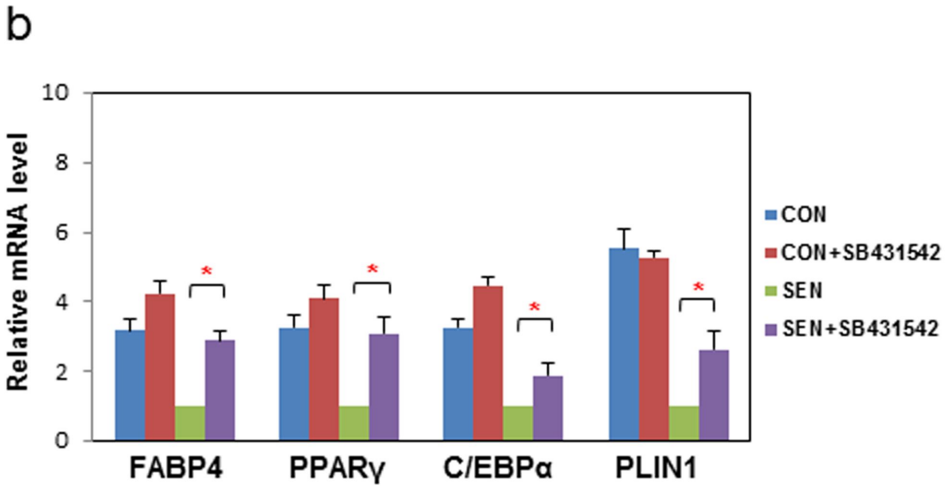
b
Relative mRNA level
10
8
6
4
2
0
FABP4
PPARγ
C/EBPα
PLIN1
CON
CON+SB431542
SEN
SEN+SB431542

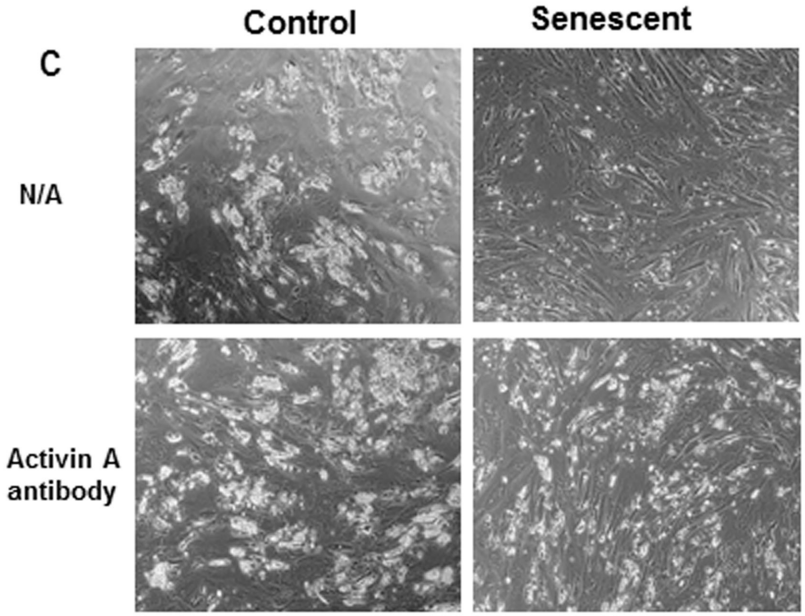
c
Control
Senescent
N/A
Activin A antibody

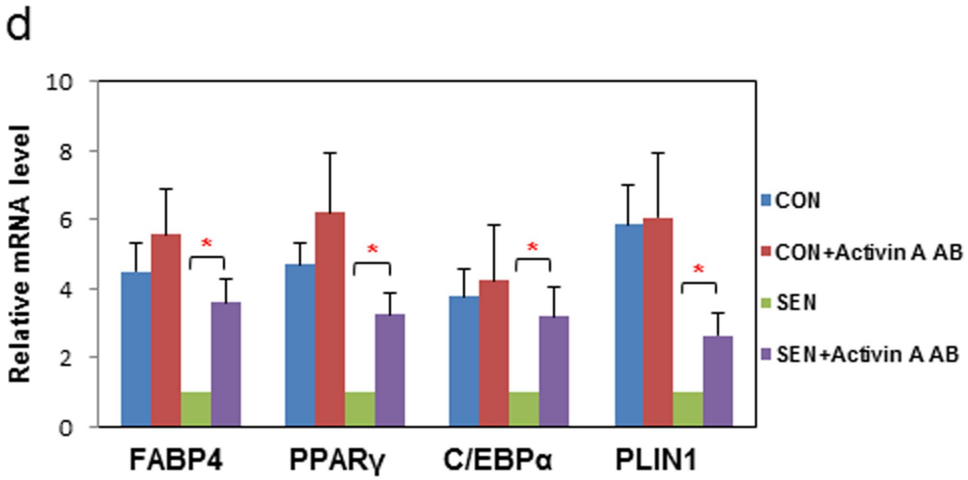
d
Relative mRNA level
10
8
6
4
2
0
FABP4
PPARγ
C/EBPα
PLIN1
CON
CON+Activin A AB
SEN
SEN+Activin A AB

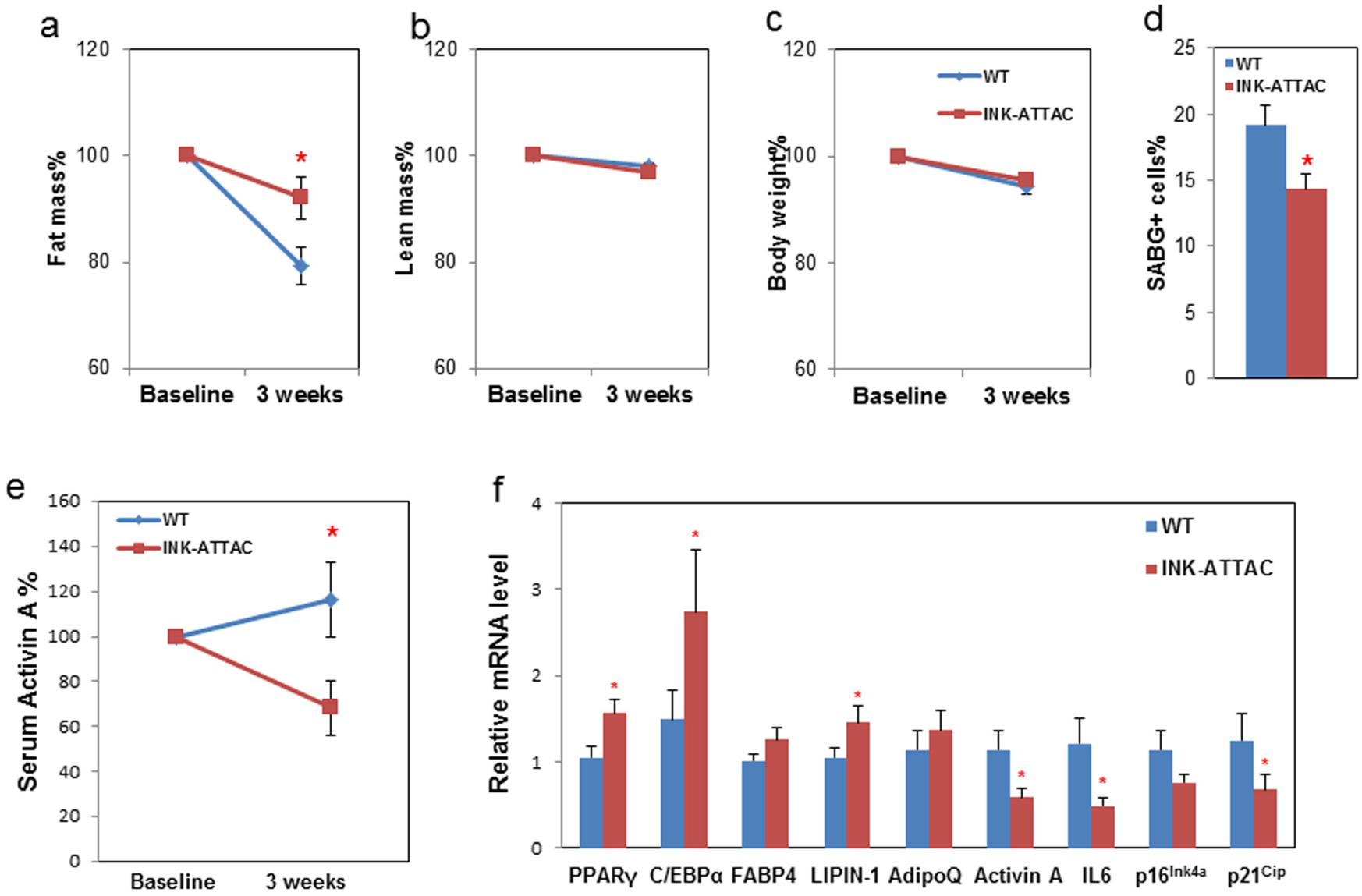
a
Fat mass%
120
100
80
60
Baseline
3 weeks
*
b
Lean mass%
120
100
80
60
Baseline
3 weeks
c
Body weight%
120
100
80
60
Baseline
3 weeks
WT
INK-ATTAC
d
SABG+ cells%
25
20
15
10
5
0
WT
INK-ATTAC
*
e
Serum Activin A %
160
140
120
100
80
60
40
20
0
WT
INK-ATTAC
*
Baseline
3 weeks
f
Relative mRNA level
4
3
2
1
0
WT
INK-ATTAC
PPARγ
C/EBPα
FABP4
LIPIN-1
AdipoQ
Activin A
IL6
p16Ink4a
p21Cip

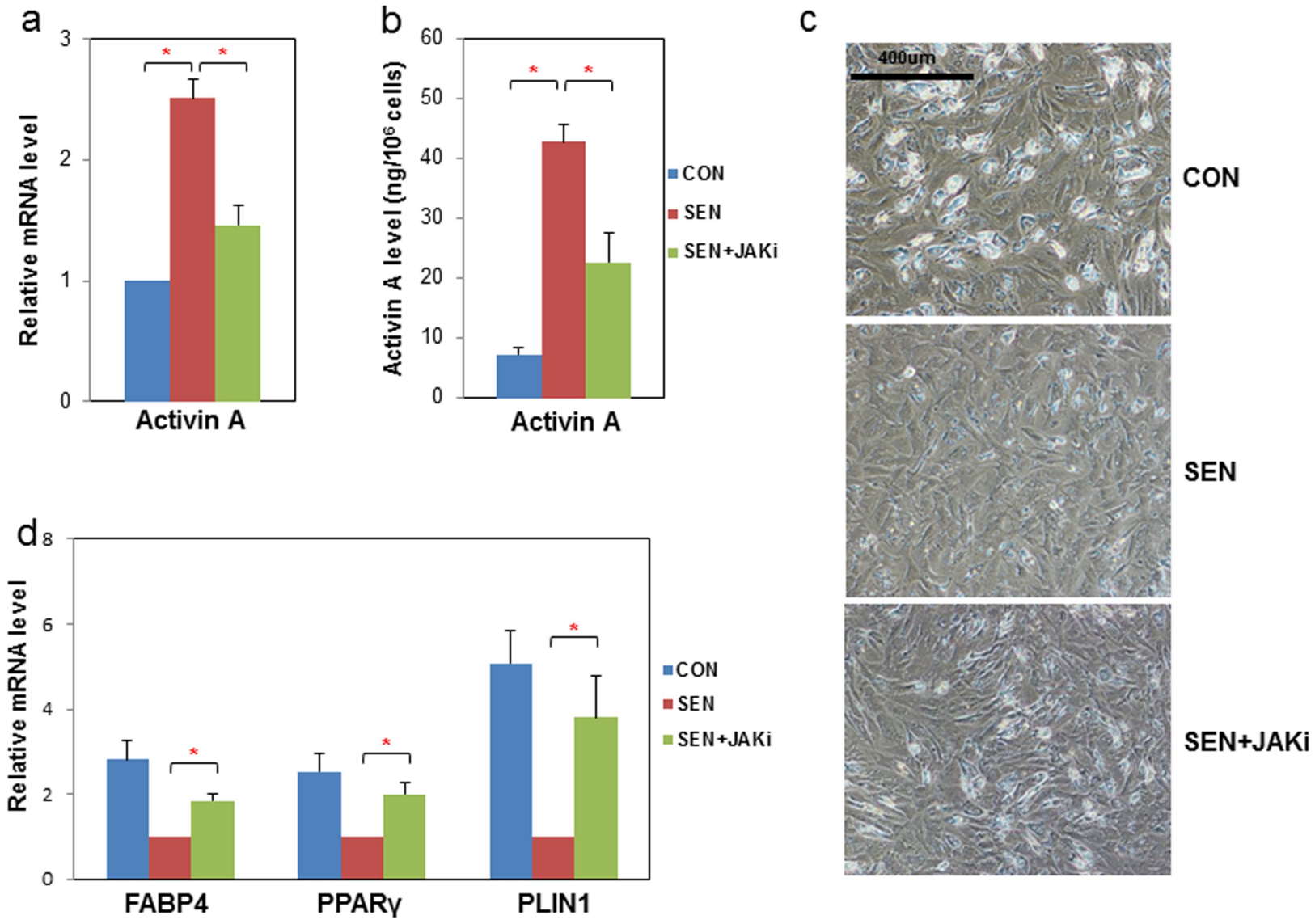
a
Relative mRNA level
3
2
1
0
*
*
Activin A
b
Activin A level (ng/10⁶ cells)
60
50
40
30
20
10
0
*
*
Activin A
CON
SEN
SEN+JAKi
c
400um
CON
SEN
SEN+JAKi
d
Relative mRNA level
8
6
4
2
0
*
*
*
FABP4
PPARγ
PLIN1
CON
SEN
SEN+JAKi

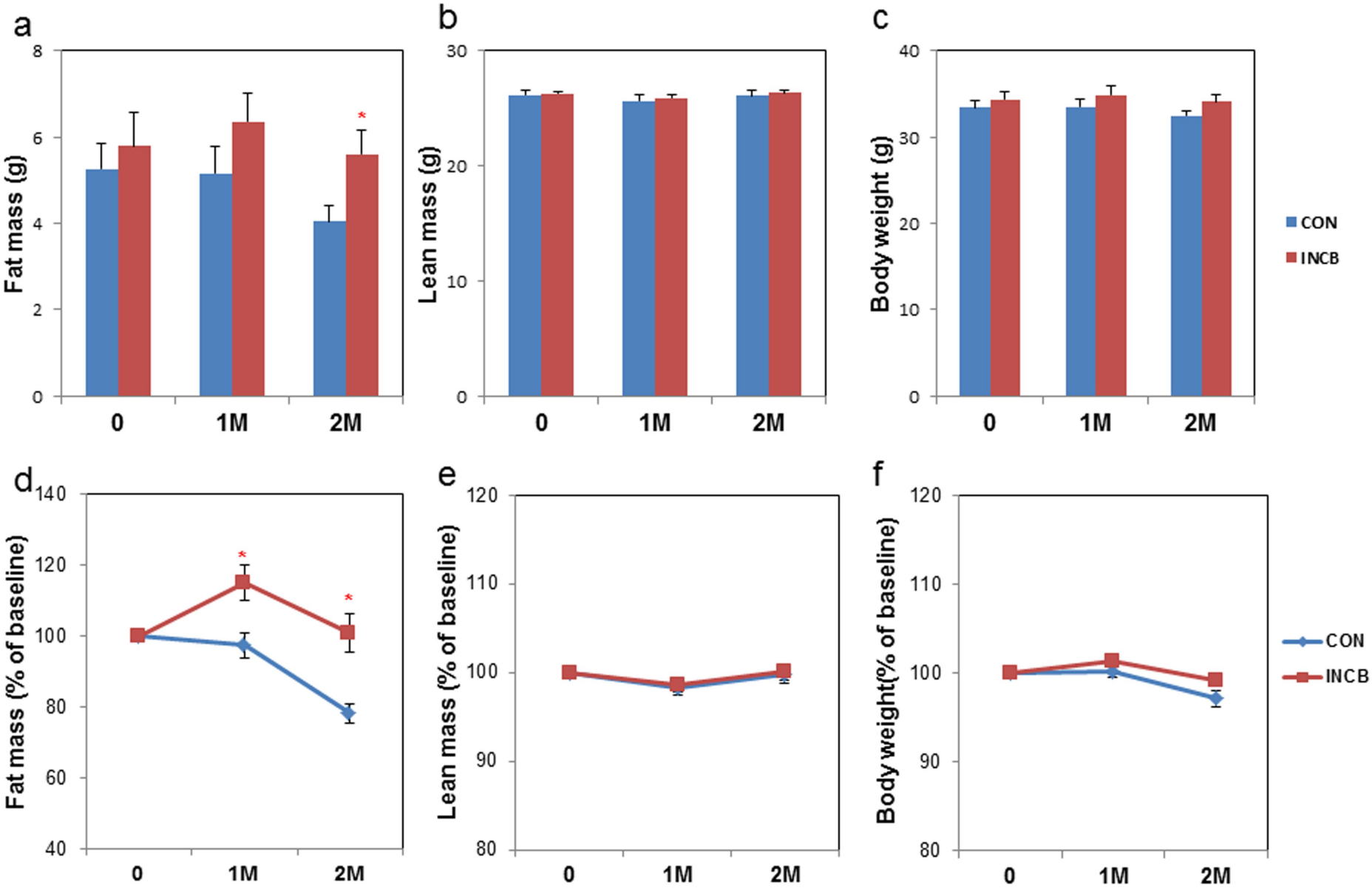
a
Fat mass (g)
8
6
4
2
0
*
0
1M
2M
b
Lean mass (g)
30
20
10
0
0
1M
2M
c
Body weight (g)
40
30
20
10
0
0
1M
2M
CON
INCB
d
Fat mass (% of baseline)
140
120
100
80
60
40
*
*
0
1M
2M
e
Lean mass (% of baseline)
120
110
100
90
80
0
1M
2M
f
Body weight(% of baseline)
120
110
100
90
80
0
1M
2M
CON
INCB

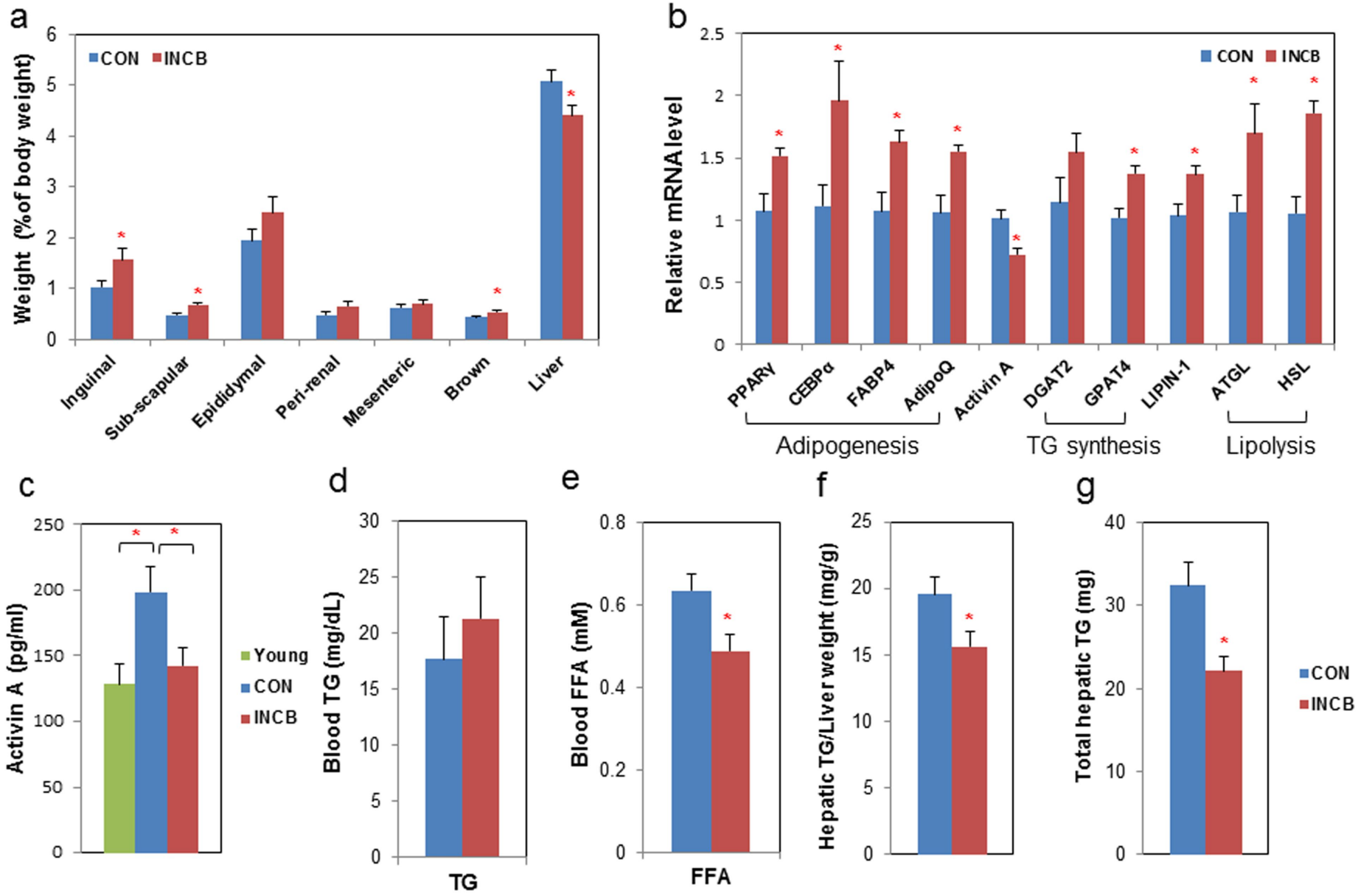
a
Weight (%of body weight)
CON
INCB
Inguinal
Sub-scapular
Epididymal
Peri-renal
Mesenteric
Brown
Liver
b
Relative mRNA level
CON
INCB
PPARγ
CEBPα
FABP4
AdipoQ
Activin A
DGAT2
GPAT4
LIPIN-1
ATGL
HSL
Adipogenesis
TG synthesis
Lipolysis
c
Activin A (pg/ml)
Young
CON
INCB
d
Blood TG (mg/dL)
TG
e
Blood FFA (mM)
FFA
f
Hepatic TG/Liver weight (mg/g)
g
Total hepatic TG (mg)
CON
INCB

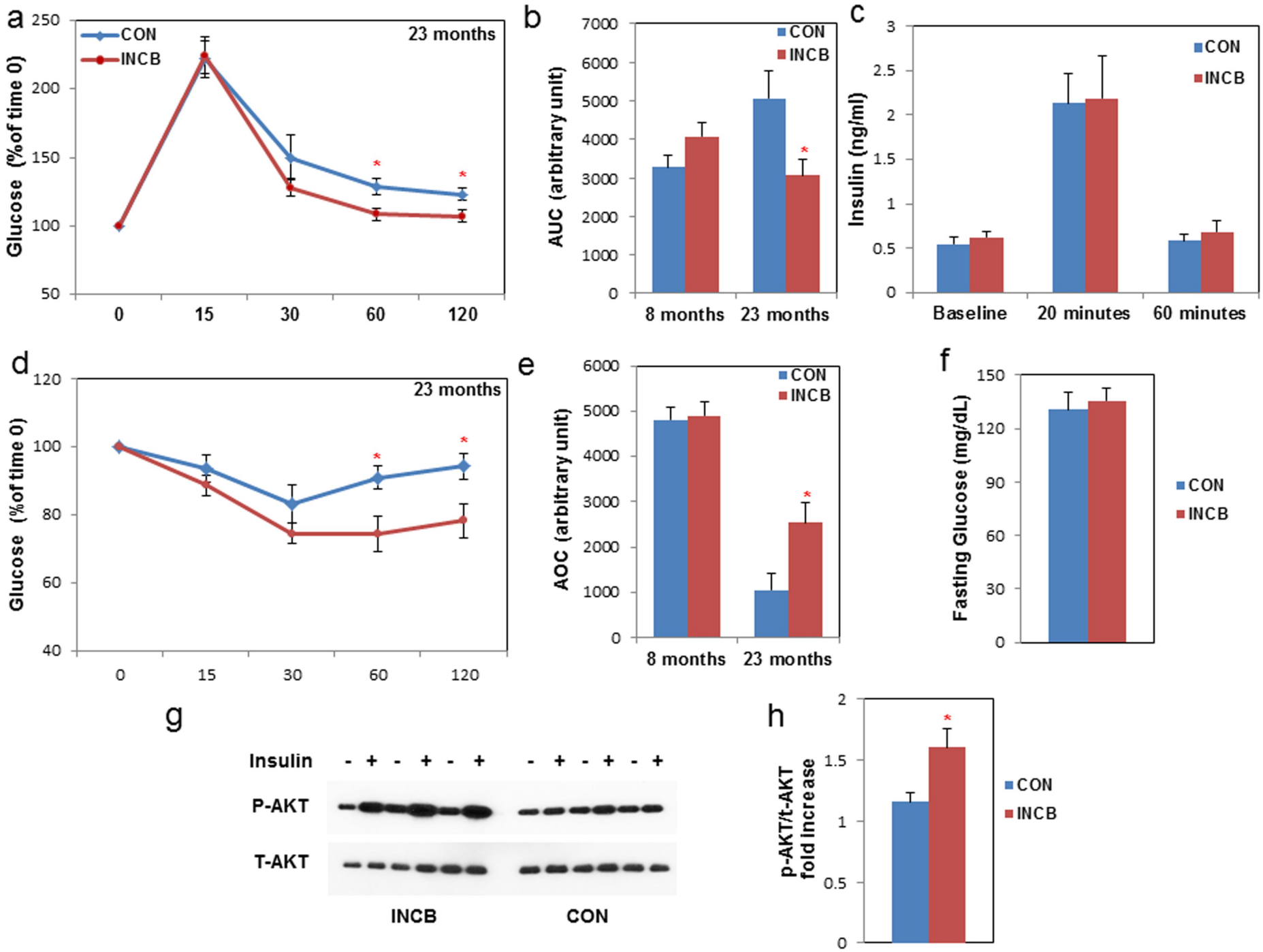
a
CON
INCB
23 months
Glucose (%of time 0)
250
200
150
100
50
0
15
30
60
120
b
CON
INCB
AUC (arbitrary unit)
7000
6000
5000
4000
3000
2000
1000
0
8 months
23 months
c
CON
INCB
Insulin (ng/ml)
3
2.5
2
1.5
1
0.5
0
Baseline
20 minutes
60 minutes
d
23 months
Glucose (%of time 0)
120
100
80
60
40
0
15
30
60
120
e
CON
INCB
AOC (arbitrary unit)
6000
5000
4000
3000
2000
1000
0
8 months
23 months
f
Fasting Glucose (mg/dL)
150
120
90
60
30
0
CON
INCB
g
Insulin
- + - + - +
- + - + - +
P-AKT
T-AKT
INCB
CON
h
p-AKT/t-AKT fold increase
2
1.5
1
0.5
0
CON
INCB